PCT WORLD INTELLECTUAL PROPERTY ORGANIZATION
International Bureau

INTERNATIONAL APPLICATION PUBLISHED UNDER THE PATENT COOPERATION TREATY (PCT)

(51) International Patent Classification 6 : G06K 9/00 | A1

(11) International Publication Number: **WO 96/27846**

(43) International Publication Date: 12 September 1996 (12.09.96)

(21) International Application Number: PCT/US96/02439

(22) International Filing Date: 4 March 1996 (04.03.96)

(30) Priority Data:
08/398,307 3 March 1995 (03.03.95) US

(71) Applicant: ARCH DEVELOPMENT CORPORATION [US/US]; The University of Chicago, 1101 East 58th Street W213, Chicago, IL 60637 (US).

(72) Inventors: BICK, Ulrich; Dept. of Radiology, 1101 East 58th Street W213, Chicago, IL 60637 (US). GIGER, Maryellen, L.; 265 Claremont, Elmhurst, IL 60126 (US).

(74) Agents: KUESTERS, Eckhard, H. et al.; Oblon, Spivak, McClelland, Maier & Neustadt, P.C., Crystal Square Five, 4th floor, 1755 Jefferson Davis Highway, Arlington, VA 22202 (US).

(81) Designated States: AL, AM, AT, AU, AZ, BB, BG, BR, BY, CA, CH, CN, CZ, DE, DK, EE, ES, FI, GB, GE, HU, IS, JP, KE, KG, KP, KR, KZ, LK, LR, LS, LT, LU, LV, MD, MG, MK, MN, MW, MX, NO, NZ, PL, PT, RO, RU, SD, SE, SG, SI, SK, TJ, TM, TR, TT, UA, UG, UZ, VN, ARIPO patent (KE, LS, MW, SD, SZ, UG), Eurasian patent (AM, AZ, BY, KG, KZ, MD, RU, TJ, TM), European patent (AT, BE, CH, DE, DK, ES, FI, FR, GB, GR, IE, IT, LU, MC, NL, PT, SE), OAPI patent (BF, BJ, CF, CG, CI, CM, GA, GN, ML, MR, NE, SN, TD, TG).

Published
With international search report.

(54) Title: METHOD AND SYSTEM FOR THE DETECTION OF LESIONS IN MEDICAL IMAGES

(57) Abstract

A method and system for the automated detection of lesions in the medical images. Medical images, such as mammograms are segmented and optionally processing with peripheral enhancement and/or modified median filtering. A modified morphological open operation (104-106) and filtering with a modified mass filter (107-109) are performed for the initial detection of circumscribed lesions. Then, the lesions are matched using a deformable shape template with Fourier descriptors (110-112). Characterization of the match is done using simulated annealing, and measuring the circularity and density characteristics of the suspected lesion. The procedure is performed iteratively at different spatial resolution in which at each resolution step a specific lesion size is detected. The detection of the lesion leads to a localization of a suspicious region and thus the likelyhood of cancer.

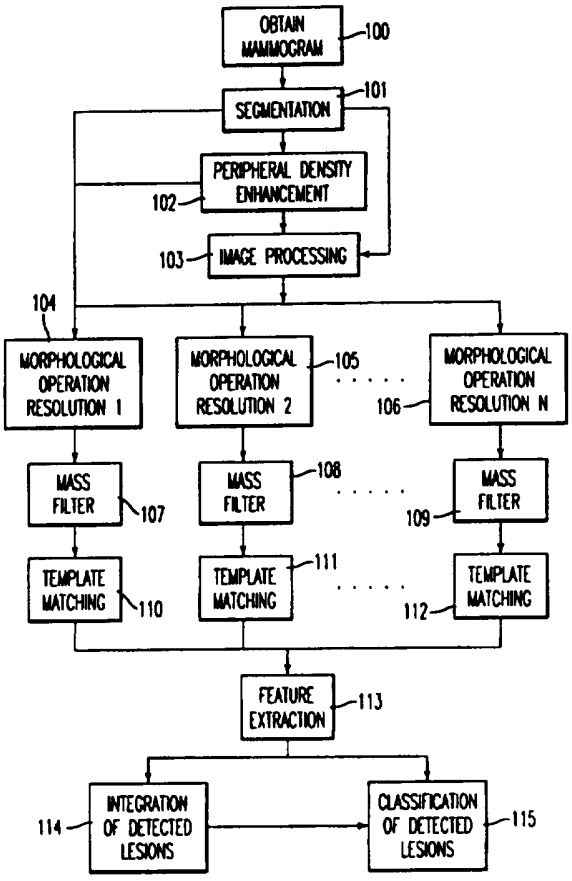

FOR THE PURPOSES OF INFORMATION ONLY

Codes used to identify States party to the PCT on the front pages of pamphlets publishing international applications under the PCT.

AM	Armenia	**GB**	United Kingdom	**MW**	Malawi
AT	Austria	**GE**	Georgia	**MX**	Mexico
AU	Australia	**GN**	Guinea	**NE**	Niger
BB	Barbados	**GR**	Greece	**NL**	Netherlands
BE	Belgium	**HU**	Hungary	**NO**	Norway
BF	Burkina Faso	**IE**	Ireland	**NZ**	New Zealand
BG	Bulgaria	**IT**	Italy	**PL**	Poland
BJ	Benin	**JP**	Japan	**PT**	Portugal
BR	Brazil	**KE**	Kenya	**RO**	Romania
BY	Belarus	**KG**	Kyrgystan	**RU**	Russian Federation
CA	Canada	**KP**	Democratic People's Republic of Korea	**SD**	Sudan
CF	Central African Republic			**SE**	Sweden
CG	Congo	**KR**	Republic of Korea	**SG**	Singapore
CH	Switzerland	**KZ**	Kazakhstan	**SI**	Slovenia
CI	Côte d'Ivoire	**LI**	Liechtenstein	**SK**	Slovakia
CM	Cameroon	**LK**	Sri Lanka	**SN**	Senegal
CN	China	**LR**	Liberia	**SZ**	Swaziland
CS	Czechoslovakia	**LT**	Lithuania	**TD**	Chad
CZ	Czech Republic	**LU**	Luxembourg	**TG**	Togo
DE	Germany	**LV**	Latvia	**TJ**	Tajikistan
DK	Denmark	**MC**	Monaco	**TT**	Trinidad and Tobago
EE	Estonia	**MD**	Republic of Moldova	**UA**	Ukraine
ES	Spain	**MG**	Madagascar	**UG**	Uganda
FI	Finland	**ML**	Mali	**US**	United States of America
FR	France	**MN**	Mongolia	**UZ**	Uzbekistan
GA	Gabon	**MR**	Mauritania	**VN**	Viet Nam

TITLE OF THE INVENTION

METHOD AND SYSTEM FOR THE DETECTION OF LESIONS IN MEDICAL IMAGES

BACKGROUND OF THE INVENTION

Field of the Invention

The invention relates generally to a method and system for an improved computerized, automatic detection and characterization of lesions in medical images, and more particularly to the detection of circumscribed masses in digital mammograms. Novel techniques in the localization (segmentation) and detection of masses in mammograms, include initially processing with peripheral equalization (correction), a modified median filter, a modified morphological open operation, filtering with a modified mass filter for the initial detection of circumscribed densities, matching using a deformable shape template with Fourier descriptors, optimization of the match using simulated annealing, and measuring the circularity and density characteristics of the suspected lesion to distinguish true positives from false positives and malignant lesions from benign lesions. The procedure is performed iteratively at different spatial resolution in which at each resolution step a specific lesion size is detected. The detection of the mass leads to a localization of a suspicious region and thus the likelihood of cancer.

Discussion of the Background

Although mammography is currently the best method for the detection of breast cancer, between 10-30% of women who have breast cancer and undergo mammography have negative mammograms. In approximately two-thirds of these false-

negative mammograms, the radiologist failed to detect the cancer that was evident retrospectively. The missed detections may be due to the subtle nature of the radiographic findings (i.e., low conspicuity of the lesion), poor image quality, eye fatigue or oversight by the radiologists. In addition, it has been suggested that double reading (by two radiologists) may increase sensitivity. It is apparent that the efficiency and effectiveness of screening procedures could be increased by using a computer system, as a "second opinion or second reading", to aid the radiologist by indicating locations of suspicious abnormalities in mammograms. In addition, mammography is becoming a high volume x-ray procedure routinely interpreted by radiologists.

If a suspicious region is detected by a radiologist, he or she must then visually extract various radiographic characteristics. Using these features, the radiologist then decides if the abnormality is likely to be malignant or benign, and what course of action should be recommended (i.e., return to screening, return for follow-up or return for biopsy). Many patients are referred for surgical biopsy on the basis of a radiographically detected mass lesion or cluster of microcalcifications. Although general rules for the differentiation between benign and malignant breast lesions exist, considerable misclassification of lesions occurs with current radiographic techniques. On average, only 10-20% of masses referred for surgical breast biopsy are actually malignant. Thus, another aim of computer use is to extract and analyze the characteristics of benign and

malignant lesions in an objective manner in order to aid the radiologist by reducing the numbers of false-positive diagnoses of malignancies, thereby decreasing patient morbidity as well as the number of surgical biopsies performed and their associated complications.

SUMMARY OF THE INVENTION

Accordingly, an object of this invention is to provide a method and system for detecting, classifying, and displaying masses in medical images of the breast.

Another object of this invention is to provide an automated method and system for the detection and/or classification of masses based on a multi-resolution analysis of mammograms.

Another object of this invention is to provide an automated method and system for the detection and/or classification of masses based on a modified morphological open operation, filtering with a modified mass filter for the initial detection of circumscribed densities, matching using a deformable shape template with Fourier descriptors, optimization of the match using simulated annealing, and measuring the circularity and density characteristics of the suspected lesion.

These and other objects are achieved according to the invention by providing a new and improved automated method and system in which a segmentation of densities (masses) within a mammogram is performed followed by optimal characterization.

BRIEF DESCRIPTION OF THE DRAWINGS

A more complete appreciation of the invention and many of the attendant advantages thereof will be readily obtained as the same becomes better understood by the reference to the following detailed description when considered in connection with the accompanying drawings, wherein:

FIGS. 1A-1C are schematic diagram illustrating embodiments of the automated method for the detection of lesions according to the invention;

FIG. 2 is a graph illustrating the step of peripheral enhancement according to the invention;

FIG. 3A is a schematic diagram of the modified median filtering according to the invention;

FIG. 3B is a schematic diagram of the modified morphological open operation according to the invention;

FIGS. 3C and 3D are graphs illustrating the criteria used in the modified morphological open operation of FIG. 3B;

FIG. 4 is a diagram illustrating the circular kernel used in the modified mass filter;

FIG. 5 is a diagram illustrating a gradient vector in the modified mass filtering;

FIG. 6 is a diagram illustrating examples of the deformable templates corresponding to the possible shapes assigned to localized densities from the Fourier descriptors analysis;

FIG. 7 is a diagram of calculating a gradient in a region of interest;

FIG. 8 is a schematic diagram illustrating the analysis

of a suspected lesion;

FIGS. 9A and 9B are tables illustrating the relationship between pixel size of the image and the lesion size being detected, and the relationship between kernel size and the lesion size being detected, respectively;

FIG. 10 is a schematic diagram of the changing of the kernel size in mass filtering;

FIG. 11 is a diagram of two detected lesions;

FIGS. 12A-12F illustrate examples of (12A) an original mammogram, (12B) after border segmentation, (12C) after the modified open operation, (12D) after the modified mass filter, (12E) after template matching and (12F) after feature extraction;

FIGS. 13A-13F illustrate examples of (13A) a mammogram, after peripheral enhancement, (13B) after morphological filtering, (13C) a image of the difference of the images of FIGS. 13A and 13B, and (13D-13F) after morphological filtering with pixel sizes of 1, 2 and 4 mm;

FIGS. 14A-14C illustrate (14A) an artificial lesion, (14B) its detection results, and (14C) the edge maps used in the detection;

FIG. 15A shows the location of a region of interest (ROI) used for feature analysis;

FIGS. 15B-15D show enlargement of the ROI of FIG. 15A, a truth margin, and detection results, respectively;

FIG. 16 is a graph illustrating the performance of the method in the detection of malignant lesions in a screening mammographic database; and

FIG. 17 is a schematic block diagram illustrating a system for implementing the automated method for the detection of lesions in medical images.

DETAILED DESCRIPTION OF THE PREFERRED EMBODIMENTS

Referring now to the drawings, and more particularly to FIGS. 1A-1C thereof, schematic diagrams of the automated method for the detection and classification of lesions in breast images is shown. In FIG. 1A a first embodiment of the overall scheme includes an initial acquisition of a mammogram and digitization (step 100). Next, the breast border is segmented from the rest of the image area (step 101) and peripheral density enhancement is performed on the image (step 102). The image is processed (step 103) and then subjected to a modified morphological open operation using different filter sizes (steps 104-106). The image after the open operation is mass filtered (steps 107-109) and template matched (steps 110-112). Feature extraction is then performed (step 113) followed by integration (step 114) and classification (step 115) of the detected lesions.

The method of detecting circumscribed masses according to the invention uses an automatically segmented mammographic image idicating only the actual breast region (step 101) after an optional application of the peripheral density equalization (step 102). Segmentation of a mammogram is described in application Serial No. 08/158,320 to Bick et al, the disclosure of which is herein incorporated by reference.

In the segmentation process, noise filtering is applied

tc the digital mammogram followed by application of the gray-value range operator. Using information from the local range operator a modified global histogram analysis is performed. Region growing is performed on the threshold image using connectivity (counting pixels), followed by a morphological erosion operation. The distance map of the image is determined and the boundary of the segmented object (breast) in the image is then tracked to yield its contour. The contour can then be output onto the digital image or passed to other computer algorithms.

Note that there is an inverse relationship between gray level and optical density. A low optical density (white region) on the mammogram (high anatomic density) corresponds to a high gray level (1023), whereas a high optical density (black region) on the mammogram corresponds to a low gray level (0).

The image after segmenting can be processed (step 103) or peripheral density enhancement can be performed. Peripheral density enhancement is described in application Serial No. 08/158,320. The average gray values of the pixels as a function of distance from the breast border. An enhancement curve is determined by fitting, such as polynomial fitting, a curve of the average gray values as a function of distance, and then reversing the fit. The enhancement curve is added to the curve of the average gray values as a function of distance to produce an enhanced gray value curve. This results in a peripherally enhanced image where the center and the portion near the border are simultaneously displayed without loss in

contrast. FIG. 2 shows the curve of the average gray values as a function of distance, the reversed fitted curve and the peripherally enhanced curve.

The segmented image, with or without peripheral density enhancement, is then optionally processed (step 103). An initial modified median filter of size nxn may be used to eliminate isolated aberrant (very dark, low gray level) pixel values in the segmented image, since this would disturb the erosion step. The modified median filtering is shown in FIG. 3A. The median filter can be of 3x3 size, for example. The conventional median filter is described in, for example, "The Image Processing Handbook," 2nd Ed., by John Russ (CRC Press 1995).

At a beginning pixel location l(x,y) in the image (step 300), which can be either the segmented or the peripherally enhanced segmented image, the local minimum is determined (step 301) in the surrounding neighborhood (nxn pixels). If the gray level at pixel location l(x,y) is smaller than the local minimum by a certain number of gray levels (M) in step 302, then that gray level is corrected by the median filter (step 303). An example of M is 5 gray levels, but other values are possible. In the embodiment, the gray level of the pixel at l(x,y) is updated to the median pixel value of the neighborhood.

It is checked whether the pixel is the last pixel for processing (step 304). If no, the next pixel is selected (step 305) and step 301 is repeated. If the answer in step 302 is no, the process moves to step 304. When the last pixel

location is reached (step 304), the filtering is completed for all of the pixels in the image.

Two criteria are then used to control which pixels are used as seed pixels for the morphological operation, to preserve the gray value characteristics of larger lesions as far as possible. As shown in FIG. 3B, beginning at pixel location I(x,y) (step 310) a check is made to determine whether pixel I(x,y) is a seed pixel. The local maximum of the neighborhood is calculated (step 311).

To qualify as a seed pixel the following criteria must be fulfilled. First, there must be a negative Laplacian (gray value of the pixel in question minus the local minimum gray value must be less than the local maximum gray value minus the gray value of the pixel in question, (step 312). This, as demonstrated in FIGS. 3C and 3D, prevents erosion of the center of a small mass. In FIG. 3C the gray value I(x,y)=MAX, so no change is made to pixel value and the center is preserved. In FIG. 3D, I(x,y)-MIN < MAX-I(x,y), so the gray value of pixel at location I(x,y) is changed.

Second, only pixels with a small distance from the local minimum are used as erosion centers (step 313). That is, the location of the seed pixel must be close to the location of the local MIN. This preserves the gray value slope in the periphery of larger lesions. An example of the distance is 3 pixels, and other values may be chosen.

If the answer is no at either of steps 312 and 313, the next pixel is selected (step 314) and the process is repeated. For those pixels which qualify as a seed pixel, the

morphological open operation is performed (step 315).

The morphological open (erosion followed by dilation) shown in FIG. 3B is performed on the segmented image, with or without modified median filtering, as shown in FIG. 1A. The morphological open operation is also described in Russ, supra. Only the erosion processing can be performed, omitting the dilation procedure. The main effect of the erosion is smoothing of the image while keeping lesions that are of interest. The main effect of the dilation is to return masses to roughly their original size. The dilation is optional.

The structuring element in the embodiment for the morphological operation is a circle with a diameter of 7 pixels, e.g. for a pixel size of 0.5 mm. The structuring eliminates small circular and thin linear structures up to a diameter of 3.5 mm (for a 0.5 mm pixel size). If larger structuring elements are used, the subsequently used mass filter size is changed (as discussed below). At the same time irregular densities are rounded by this process.

This morphological operation is different from the conventional operation in the sense that a threshold E is used to control how much structure is eroded. If the difference, i.e. the gray level value of a pixel in the image prior to the morphological operation, I(x,y), minus the gray level value after the morphological operation, P(x,y), is larger than the threshold E (step 316), then the gray level value of the pixel is replaced by the output of the morphological operation (step 317). Examples of E can range from 0-10 in terms of gray levels. When dilation is performed, if the gray level after

dilation exceeds the original gray level of the pixel, the original gray level value is used for the pixel. This is repeated for all pixels.

Referring to FIG. 1A, the morphological step is performed at different image resolutions. For example, resolution 1 (step 104) can use an image having a 0.5 mm pixel size (resolution 1), with the image being 512x512 pixels. The process is repeated in parallel for images having 1 mm, 1.5 mm, 2.5 mm, etc. pixel size with a corresponding decrease in image size as the pixel size increase (for 1.0 mm pixel size, the image is 256x256, etc.).

The process can also be conducted serially with a change in the resolution for each iteration. A second embodiment of the method according to the invention is shown in FIG. 1B. After steps 100-103, the morphological operation is performed at a beginning resolution (step 104), followed by mass filtering (step 107) and template matching (step 110). The image resolution is changed in step 116 and the results of the matching are stored in step 117. It then determined whether the maximum resolution has been exceeded (step 118). If no, the process is repeated at the new resolution. If yes, feature extraction, integration and classification (steps 113-115) are performed the same as in FIG. 1A.

FIG. 1C shows a third embodiment of the invention. The method shown in FIG. 1C differs from the method shown in FIG. 1B in that a thresholding operation 119 is performed using the output of the mass filtering step. The mass filtered image identifies areas suspected of containing a lesion that can be

further processed by gray-level thresholding. After thresholding the image with the remaining suspected lesions is input to step 113 for feature analysis, followed by steps 114 and 115, as in the method of FIG. 1B.

FIG. 4 is a diagram illustrating the circular kernel used in the mass filter. For detection of circumscribed densities a mass filter with a circular base is used (this mass filter is a modified IRIS filter; for a description of the IRIS filter see Kobatake et al., CAR 1993: pp 624-629). The kernel is ring-shaped (pixels 402) around a center pixel 400. Note in this kernel that the center pixel locations 401 are absent since they would not contribute useful values to the overall filter value (as described below). A ring-shaped filter rather than just a solid circular filter is thus used.

The mass filter value is based on the local gradient (in the embodiment a 7x7 kernel is used) in x- (Dx) and y- (Dy) directions. Differences from the description of the IRIS filter in Kobatake et al. include use of a ring-shaped filter, second derivative instead of the gradient, and edge orientation bins. Gradient values smaller than a gradient threshold (e.g., 10) are not used in the calculation of the filter value.

The edge orientation at a specific image point is equivalent to the gradient vector and the edge strength is calculated as the second derivative in edge orientation. FIG. 5 shows a gradient 500 at point 501. This assures that regions with a constant gradual slope do not contribute to the mass filter value. The gradient is oriented at an angle ϕ

relative to a radial line from point 501 to point (x,y). The filter value is calculated separately for a specific number of edge orientation bins, such as 16 (B_1, B_2...B_{16}). Orientation bins are radial sectors of the circular area. For example, each of 16 bins would cover an angle of $\pi/8$. A bin 502, shown for a sector of $\pi/8$, is made of the pixels 402 between lines 503.

The calculation for a given pixel location (x,y) is given for the calculation of each orientation bin by:

$$f(B_i) = (1/N)\,\Sigma_{P\ in\ K}[MAX(0,\cos\phi) * Edge\ Strength\ (at\ P)]$$

where:

$f(B_i)$ filter value for edge orientation bin

K filter kernel

P neighbor point in K

N number of points in K

ϕ angle between gradient vector and connection line center point/neighbor point

Edge strength is obtained from the second derivative of P calculated in edge orientation. The final filter value is calculated as sum of the individual orientation bins, where a specified number of bins j, for example 4, with the highest values are ignored. That is:

$$\text{filter value at pixel } 1(x,y) = \Sigma_{i-j}\, f(B_i)$$

for B_i not equal to the j highest bins. This prevents an influence of straight edges (e.g. the pectoralis muscle border) on the filter value, since all points along this edge are within the same orientation bin without changing the filter value for ideal circular lesions.

Usually the filter value is highest in the center of a lesion. The highest filter values are found for round or slightly oval shaped lesions. The neighborhood used in calculation of the filter value is empirically determined to be around 10 pixels (outer radius); this could be increased to improve the detection of oval shaped masses. In addition, a gradient threshold can be employed so that pixels in the neighborhood that have a gradient smaller than the threshold (e.g., 10) do not contribute to the calculation of the filter value.

The image outputted by the mass filter is then subjected to template matching. Local maxima of the filter value define potential center points of mass lesions, which are used in steps 111-113, the matching of a deformable template on to the lesion border. The edges of the suspect lesion can be obtained from the derivative or second derivative of the image output from the mass filtering. The deformable shape template is defined using Fourier descriptors. An initial shape is selected and the Fourier descriptors are varied to dynamically fit the shape of the lesion. Fourier descriptors are described in, for example Arbter et al., *Application of Affine-invariant Fourier Descriptors to Recognition of 3-D Objects*, IEEE Trans. Pattern Analysis Machine Intelligence 12:640-647 (1990); Kuhl et al., *Elliptic Fourier Features of a Closed Contour*, Computer Graphics Image Processing 18:236-258 (1982); Wallace et al., *An Efficient Three-dimensional Aircraft Recognition Algorithm Using Normalized Fourier Descriptors*, ibid., 13:99-126 (1980); Granlund, *Fourier*

Preprocessing for Hand Print Character Recognition, IEEE Trans. Computers 21:195-201 (1972); Zahn et al., *Fourier Descriptors for Plane Closed Curves*. ibid., 21:269-281 (1972); Crimmins, *A Complete Set of Fourier Descriptors for Two-dimensional Shape*, IEEE Trans. Sys. Man Cybernetics 12:848-855 (1982); Persoon et al., *Shape Discrimination Using Fourier Descriptors*, ibid., 7:170-179 (1977); and Richard et al., *Identification of Three-dimensional Objects Using Fourier Descriptors of the Boundary Curve*, ibid., 4:371-378 (1974).

In the template matching step the object contour is generated as an inverse Fourier transform of a limited number of complex Fourier terms. The following relationship exists between a closed planar curve g(l) and Fourier descriptors c_k:

g(l) planar curve and Fourier descriptors:

$$c_k = |c_k| e^{j\phi_k} = (1/L) \int_0^L g(l)\, e^{-j\pi kl/L} dl$$

where:

g(l) is a planar curve with a runlength l; the real of part of g = x coordinate, the imaginary part of g = y coordinate

c_k Fourier descriptors with $-N/2 \leq k \leq N/2$, $N \rightarrow \infty$

By variation of the terms -2, -1, 0, 1, and 2 arbitrary elliptical or kidney shape contours can be generated. The terms -2 to 2 were selected since the lesions are of simple shape. However, one can modify the terms using a priori knowledge of the lesions to be detected. The term 0 defines the position and the terms -1 and 1 define size and orientation of the main ellipse.

In the mass detection the following fourier descriptors

are used:

$c_k = 0$ for $k \ll -2$ or $k > 2$

$c_{-1} = sp_1 e^{j\alpha}$

$c_0 = x + jy$

$c_1 = se^{j\alpha}$

$c_2 = sp_2 e^{j(\alpha + \pi)}$

x x center position

y y center position

s size

α orientation (angle between main ellipse and x-axis)

p_1: variable parameter to describe the short/long axis ratio of the main ellipse with $0 \leq p_1 \leq 0.5$ (long axis: $s + sp_1$, short axis: $s - sp_1$ for $p_1 = 0$, the Fourier descriptors define a circle as a special case of an ellipse)

p_2 variable parameter to describe the degree of asymmetry (kidney shape) with $0 \leq p_2 \leq 0.3$

FIG. 6 is a diagram illustrating examples of the deformable templates corresponding to the possible shapes assigned to localized densities from the Fourier descriptors analysis discussed above, with the p_1 and p_2 values indicated for each shape. Note that the center position and the angle (orientation) and the size of each can be varied. FIG. 6 is an example of possible shapes, and the invention is not limited to these particular shapes or this number of shapes.

The lesion contour is generated by variation of the Fourier terms within a certain range with minimization of a cost function using lesion contrast, edge strength and

deviation from the ideal circular shape. This process is performed on the output from the mass filter. Simulated annealing is used for minimization.

Simulated annealing is a technique for optimization, which involves a description of possible system configurations, a generator of random changes in the configuration (i.e., the "options"), a function for minimization and a control parameter (temperature) that controls the increments of the random changes. It is described in, for example, *Numerical Recipes* by Press, et al., Cambridge Press (1988).

The configuration in the embodiment is the "correct" Fourier descriptor of an extracted contour. This configuration could be obtained as an entire curve or in radial segments of the curve using different Fourier descriptors for each segment. Once "fit", the inverse of the Fourier descriptors is performed yielding the contour. With the radial segments, only a limited number of points are generated in the inverse transformation. The changes in the configuration (i.e., the contour shape, that is the Fourier descriptor coefficients c_k) are changed by changes in the center location, the size of the "lesion", the orientation (α), the long/short axis ratio (indicating the degree of being oval) and the degree of asymmetry. The method limits the changes to these in the Fourier descriptors. Examples of the range of variation for each parameter include increments in center position by one pixel, a size range of 5 to 80 pixels in diameter with an increment of 2 pixels, and a range in α

from -360° to 360°. The function to be minimized includes a center cost index of 20 (in each direction), a size cost index of 10 and an angle cost index of 10. The starting temperature was set at 30. Upon minimizing the cost function, the difference between the "lesion" center and the "fit" center, the difference between the size of the "lesion" and the size of the "fit", the Euclidean difference between x-y position of the lesion contour and the x-y position of the fit contour, etc. are minimized. The temperature is modified (cooled) as the iterations increase so that after a specified number of iterations a downward step in the temperature is taken.

In the template matching the following can be varied: the shape in terms of Fourier descriptors, the penalty factor for deviations from the mean, the center, the angle and the size. The penalty factor is a measure based on standard deviation, i.e. a limit on the amount of deformation during the template matching.

An example of the parameter file used in the deformable template matching is shown below:

-- a shape file giving which part of the curve is used
-- start temperature for the simulated annealing
-- number of iterations
-- increments such as for incrementing the center position, the size, the angle during the simulated annealing
-- number of points generated in the inverse transformation.

Note that after the matching is successful, the final coefficients of the Fourier descriptors are used to return to the x,y domain. Thus, discontinuous margin pixels along a

"mass" will be connected. The output of the template matching is contour or a partial contour of the suspect lesion.

Sixteen edge maps can be used in the shape matching. Edge maps are obtained from the second derivative, as described above. Edge maps are used since sometimes there is only one good edge in the suspected lesion. The lesion contour is generated by variation of the Fourier terms within a certain range with minimization of a cost function using lesion contrast, edge strength and deviation from the ideal circular shape. Simulated annealing is used for minimization. In the matching one can have varied the following: the shape in terms of Fourier descriptors, the penalty factor deviations from the mean, the center, the angle and the size.

For further characterization a rectangular ROI containing the suspected lesion identified in the open, mass filtering and template matching operations is extracted from the original peripheral density enhanced image. Feature extraction and analysis is performed on the suspected lesion. Feature extraction and is described in application Serial No. 08/158,389 to Giger et al., the disclosure of which is herein incorporated by reference.

This is shown in more detail in FIG. 8. The suspected lesion from the template matching is obtained (step 800). Note that a suspected lesion from another method, by a computer or manually by an observer, can also be used as input (step 801). A region of interest (ROI) containing the suspected lesion is selected (automatically or manually) in step 802. The gradient and orientation of the ROI is

calculated in step 803, followed by a calculation of the gradient index R, contrast and elongation factor in step 804. This is shown in more detail in FIG. 7, where in an ROI 700 a gradient 701 is calculated at a point 702 in a suspected lesion 703 having a center point (x,y). The pixels in the area enclosed by dashed line 704 are those pixels that do not contribute much to the gradient index (the gray value varies more towards the edge of the suspected lesion), and may be excluded.

The radial gradient index R, defined as follows:

$$R = \frac{\sum_{P \in L} \cos\phi \sqrt{D_x^2 + D_y^2}}{\sum_{P \in L} \sqrt{D_x^2 + D_y^2}}$$

where:

R radial gradient index $-1 \leq R \leq 1$

P image point

(x,y) center of suspected lesion from template matching

L detected lesion excluding the center part

D_x gradient in x-direction

D_y gradient in y-direction

ϕ angle between gradient vector and connection line center (x,y) to P

The radial gradient index is a measure of circularity and density characteristics of the lesion. The radial gradient index approaches 1 for ideal circular lesions. This radial gradient index can be viewed as the average gradient in the radial direction normalized by the average gradient. The suspected lesion size is given by the difference between the

gray level at the center to that at the margin of the suspected lesion.

To limit the number of false positives, thresholding is performed in step 805. For example, lesions with a diameter less than some preset value (e.g. < 4 mm), a contrast less than some preset value (e.g. < 0.1 optical density) or a radial gradient less that a preset value (e.g., 0.5) are eliminated.

The features after thresholding are indicated in step 806 and can be merged using, for example, rule-based methods or an artificial neural network trained to detect and classify lesions (step 807) to eliminate further more false positives or to distinguish between malignant and benign lesions. Malignant and benign lesions will possess different R values if the maglinant lesion is highly spiculated.

The open, mass filtering and template matching are performed repeatedly with different resolutions. In each resolution step a specific lesion size is detected. FIG. 9A is a table illustrating the relationship between pixel size of the image and the lesion size being detected. The number and size of resolutions chosen depends upon the type of lesions to be detected and the amount of processing time available for detection.

The kernel size in the mass filtering can also be varied. FIG. 9B is a table showing the relationship between kernel size and the size of the lesion being detected. In the embodiments described above, a single mass filter can be chosen for the different resolutions of the open filter. In a

modification of theses embodiments, the kernel size in the mass filtering can be varied, for example as shown in FIG. 9B. The modified mass filtering step is shown in FIG. 10. The image resolution is kept constant while the kernel size is varied, the kernel size is kept constant while the image resolution is varied, or both can be varied.

In step 1000, the image from the morphological operation is obtained. The initial kernel size is set (step 1001) and the mass filtering is performed at the initial kernel size (step 1002). The image after mass filtering is stored (step 1003). Next, it is checked whether the maximum kernel size has been reached in step 1004. If no, then a new kernel size is selected (step 1005) and the mass filtering is performed again. After the last kernel size is used, the images are output (step 1006).

After features analysis has been performed, in step 116 of FIG. 1A the different detected lesions from all of the outputs obtained from different resolution images, different size kernels, or both, are integrated. Locations indicating the same lesion may show up in more than one image.

If two lesions overlap, the lesion with the smaller radial gradient index is eliminated. The amount of acceptable overlap can be varied by specifying the percent of overlap allowed. In the embodiment, 30% was chosen, but other values can be used. Referring to FIG. 11, two lesions 1100 and 1101 are shown. The smaller lesion, having the larger gradient index is kept.

FIGS. 12A-12F illustrate example of (12A) an original

mammogram, (12B) after border segmentation, (12C) after the modified open operation, (12D) after the mass filtering, (12E) after template matching and (12F) after feature extraction in which the suspect lesions are prioritized by number (with one being the most suspicious). In this case lesion 1 was an intramammary lymph node with a radial gradient index of 0.92, lesion 2 was a 10 mm invasive ductal cancer (R = 0.90), lesion 3 was a 7 mm invasive ductal cancer (R = 0.85), and lesions 4 through 7 were false positive with R ranging from 0.78 to 0.52.

In FIG. 12D the suspected lesions are evidently highlighted, allowing their extraction through thresholding as described above. FIG. 12E contains many contrast features not evident from a visual inspection of FIG. 12D. The template matching is sensitive to subtle variations in the mass-filtered image.

FIGS. 13A-13F show examples of a mammogram (13A) after peripheral enhancement and (13B) after morphological filter with a pixel size of 0.5 mm. Figure 13C shows the difference image of FIG. 13A minus FIG. 13B, illustrating the small detail, non-lesion like structures that are eliminated by the morphological operation. The effect of morphological operations with different pixel sizes is shown in FIGS. 13D-13F for pixel sizes of 1.0 mm, 2.0 mm and 4.0 mm, respectively.

FIGS. 14A-14C illustrates (14A) an artificial ideal spherical lesion and (14B) its detection results. FIG. 14C shows the 16 directional edge maps used in the method. The 16

edge maps correspond to 16 equal radial sectors making up the circular lesion. Other numbers of edge maps can be chosen.

FIG. 15A shows the location of the ROI used for feature analysis within the original mammogram after peripheral enhancement. FIGS. 15B-15D show enlargements of the ROI, the truth margin as marked by a radiologists and the detection result for lesions 1 and 2 from FIG. 12F, respectively.

Figure 16 is a graph illustrating the performance of the method in the detection of malignant lesions in a screening mammographic database in terms of FROC (free response operating characteristic) curve. For this performance evaluation, 45 invasive cancers less than 10 mm in size were used.

FIG. 17 is a schematic block diagram illustrating a system for implementing the automated method for the detection of lesions in medical images. The system of FIG. 17 operates and carries out functions as described above. A data input device 1700, such as a x-ray mammography device with a laser scanner and digitizer, produces a digitized mammogram. The digitized mammogram is segmented by segmenting circuit 1701 and then input to a peripheral enhancement circuit 1702 or sampling circuit 1703. Either the digitized mammogram or the peripherally enhanced is sampled by the sampling circuit 1703 (to select a pixel size) and then optionally processed by a modified median filter 1704. Either the output of the sampling circuit 1703 or the filter 1704 is input to and processed by morphological circuit 1705. The output of circuit 1705 is fed to mass filter circuit 1706 for mass

filtering. Next, the mass-filtered image is fed to a Fourier descriptors generating circuit 1707, edge images generating circuit 1708 and simulated annealing circuit 1709 for template matching. The image(s) are then fed to a feature analysis circuit 1710 for feature extraction and analysis. Memory 1711 is available to store images. The features are merged for classification and integration in feature merging circuit 1712, and can be displayed on display 1713, such as a video display terminal.

The images can also be transferred from memory 1711 via transfer circuit 1714 to a feature analysis circuit 1715 to perform feature extraction and analysis. The features are fed to a rule-based circuit or neural network 1716 to perform detection and classification of lesions. Superimposing circuit 1717 allows the detected lesions to be displayed on the images.

The elements of the system of FIG. 17 can be carried out in software or in hardware, such as a programmed microcomputer. The neural network can also be carried out in software or as a semiconductor layout.

Obviously, numerous modifications and variations of the present invention are possible in light of the above technique. It is therefore to be understood that within the scope of the appended claims, the invention may be practiced otherwise than as specifically described herein. Although the current application is focussed on the detection and classification of mass lesions in mammograms, the concept can be expanded to the detection and classification of

abnormalities in other organs in the human body, such as the lungs and the liver.

WHAT IS CLAIMED AS NEW AND DESIRED TO BE SECURED BY LETTERS PATENT OF THE UNITED STATES IS:

1. A method for the automated detection of mass lesions in mammographic images, comprising:

generating a mammogram;

segmenting said mammogram to produce a segmented mammogram;

performing a morphological operation on said segmented mammogram;

performing mass filtering;

performing template matching; and

detecting a lesion.

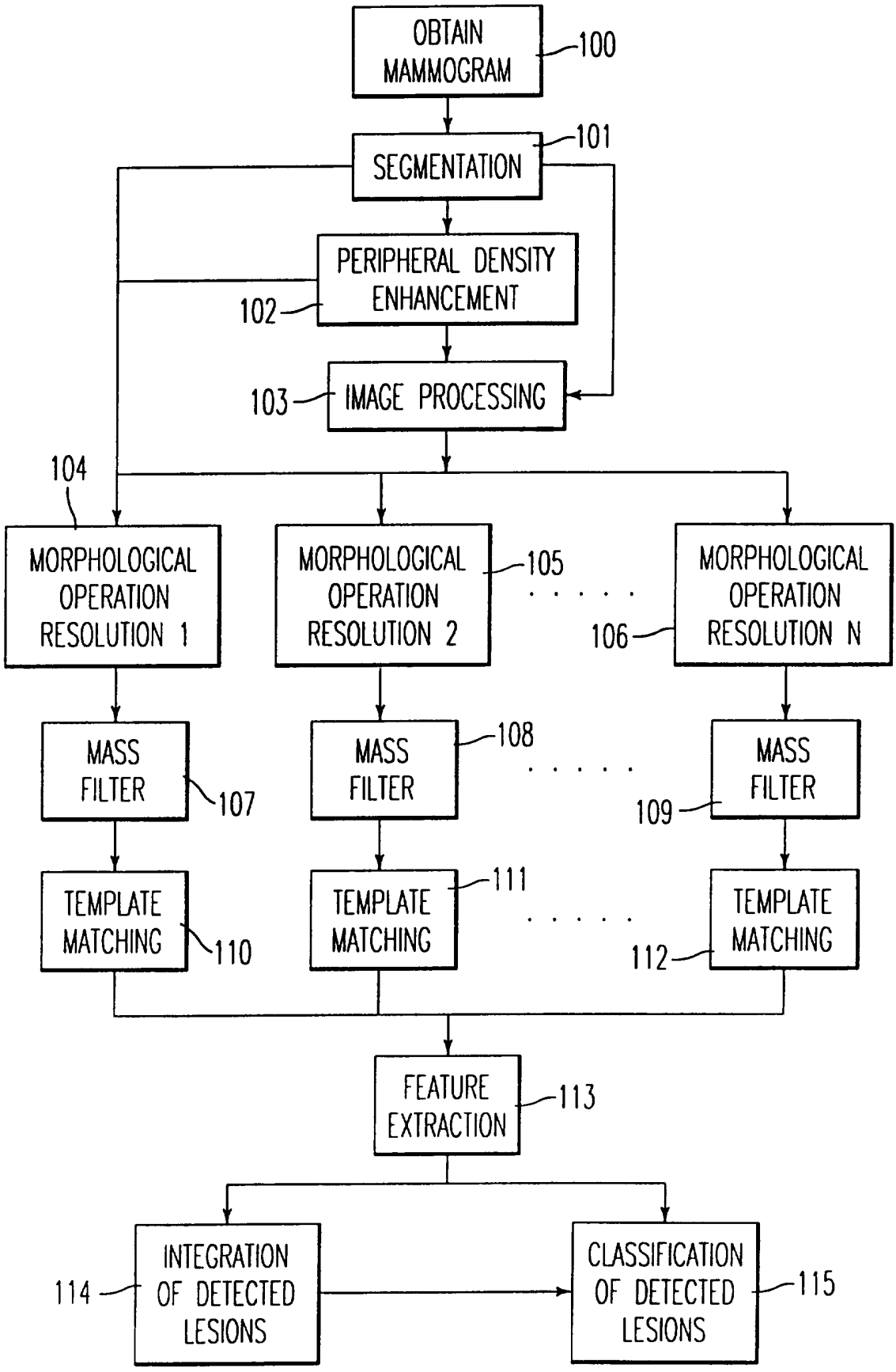
OBTAIN MAMMOGRAM
100
SEGMENTATION
101
PERIPHERAL DENSITY ENHANCEMENT
102
IMAGE PROCESSING
103
104
MORPHOLOGICAL OPERATION RESOLUTION 1
MORPHOLOGICAL OPERATION RESOLUTION 2
105
MORPHOLOGICAL OPERATION RESOLUTION N
106
MASS FILTER
107
MASS FILTER
108
MASS FILTER
109
TEMPLATE MATCHING
110
TEMPLATE MATCHING
111
TEMPLATE MATCHING
112
FEATURE EXTRACTION
113
INTEGRATION OF DETECTED LESIONS
114
CLASSIFICATION OF DETECTED LESIONS
115

FIG. 1A

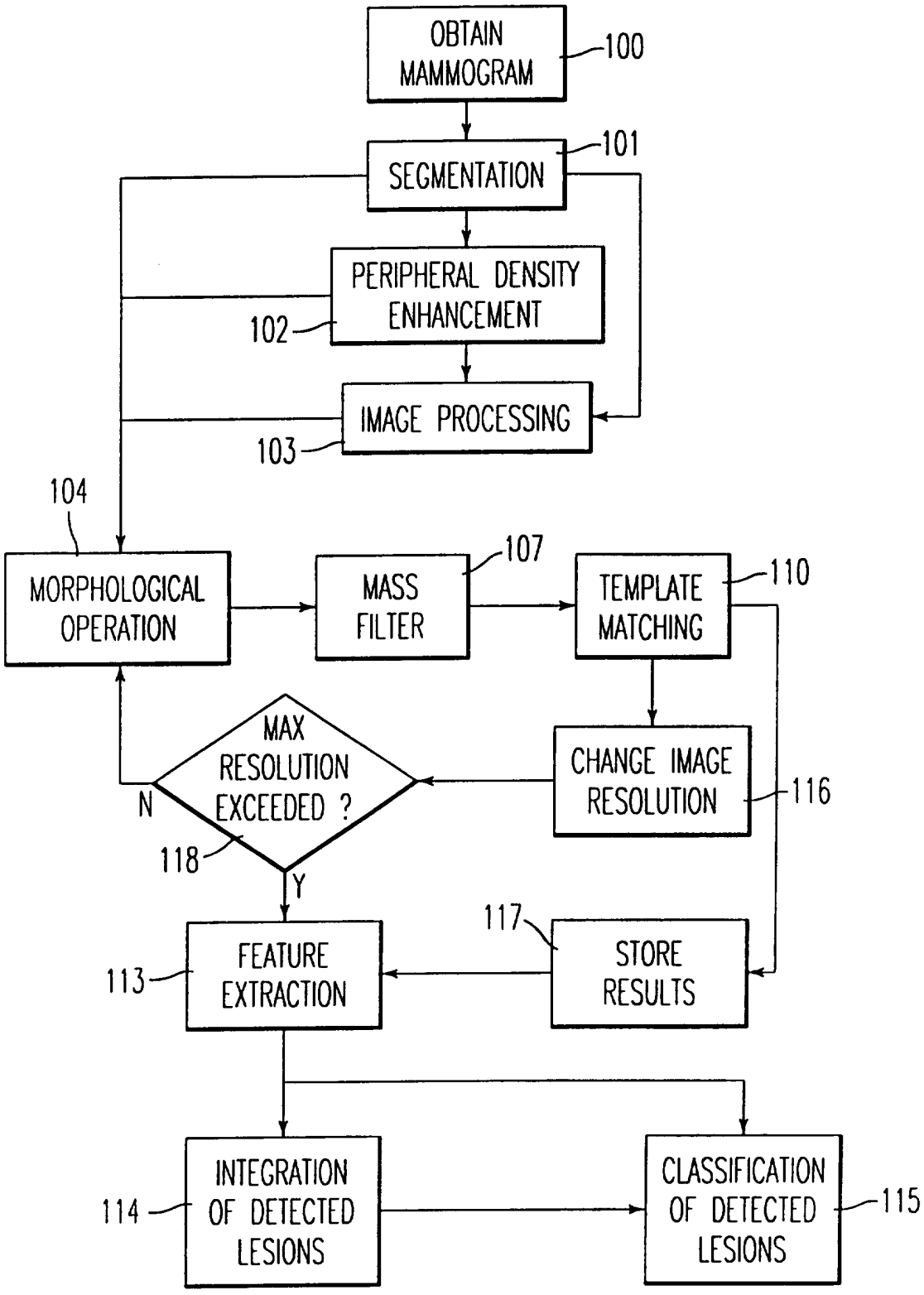
OBTAIN MAMMOGRAM
100
SEGMENTATION
101
PERIPHERAL DENSITY ENHANCEMENT
102
IMAGE PROCESSING
103
104
MORPHOLOGICAL OPERATION
MASS FILTER
107
TEMPLATE MATCHING
110
MAX RESOLUTION EXCEEDED ?
N
118
Y
CHANGE IMAGE RESOLUTION
116
117
STORE RESULTS
FEATURE EXTRACTION
113
INTEGRATION OF DETECTED LESIONS
114
CLASSIFICATION OF DETECTED LESIONS
115

FIG. 1B

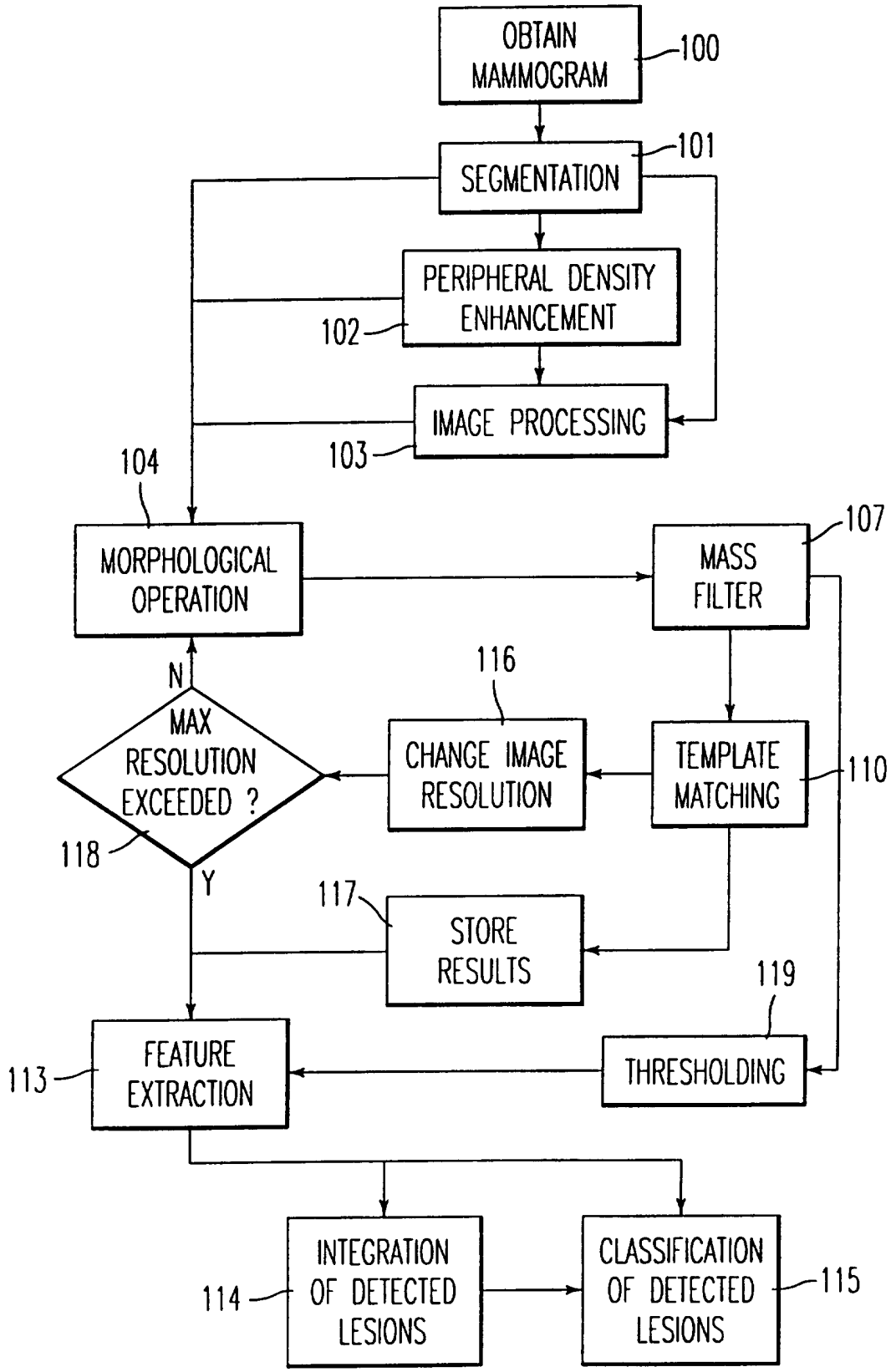
OBTAIN MAMMOGRAM
100
SEGMENTATION
101
PERIPHERAL DENSITY ENHANCEMENT
102
IMAGE PROCESSING
103
104
MORPHOLOGICAL OPERATION
MASS FILTER
107
N
MAX RESOLUTION EXCEEDED ?
118
Y
116
CHANGE IMAGE RESOLUTION
TEMPLATE MATCHING
110
117
STORE RESULTS
119
FEATURE EXTRACTION
113
THRESHOLDING
INTEGRATION OF DETECTED LESIONS
114
CLASSIFICATION OF DETECTED LESIONS
115

FIG. 1C

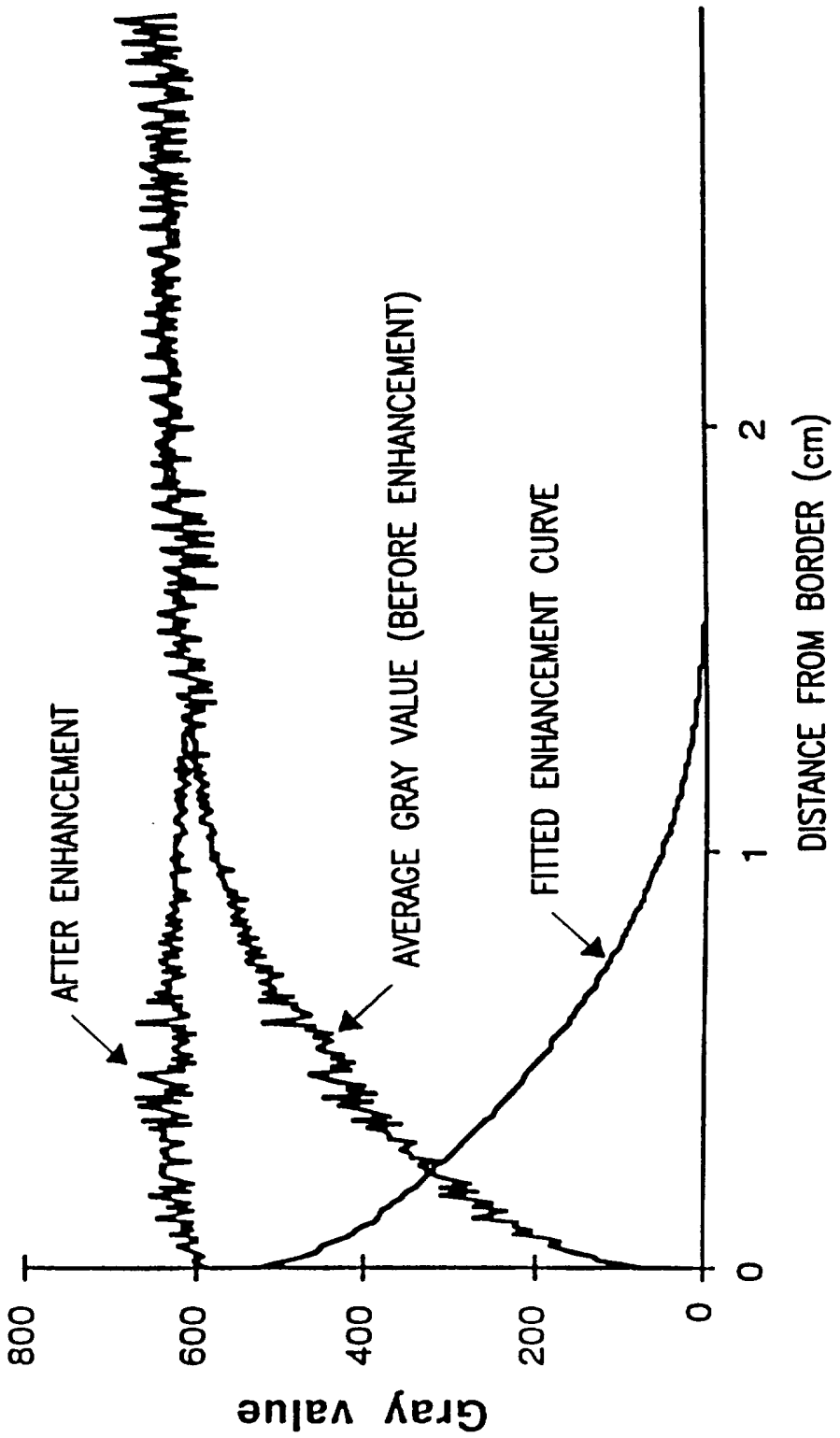
AFTER ENHANCEMENT
AVERAGE GRAY VALUE (BEFORE ENHANCEMENT)
FITTED ENHANCEMENT CURVE
Gray value
800
600
400
200
0
0
1
2
DISTANCE FROM BORDER (cm)

FIG.2

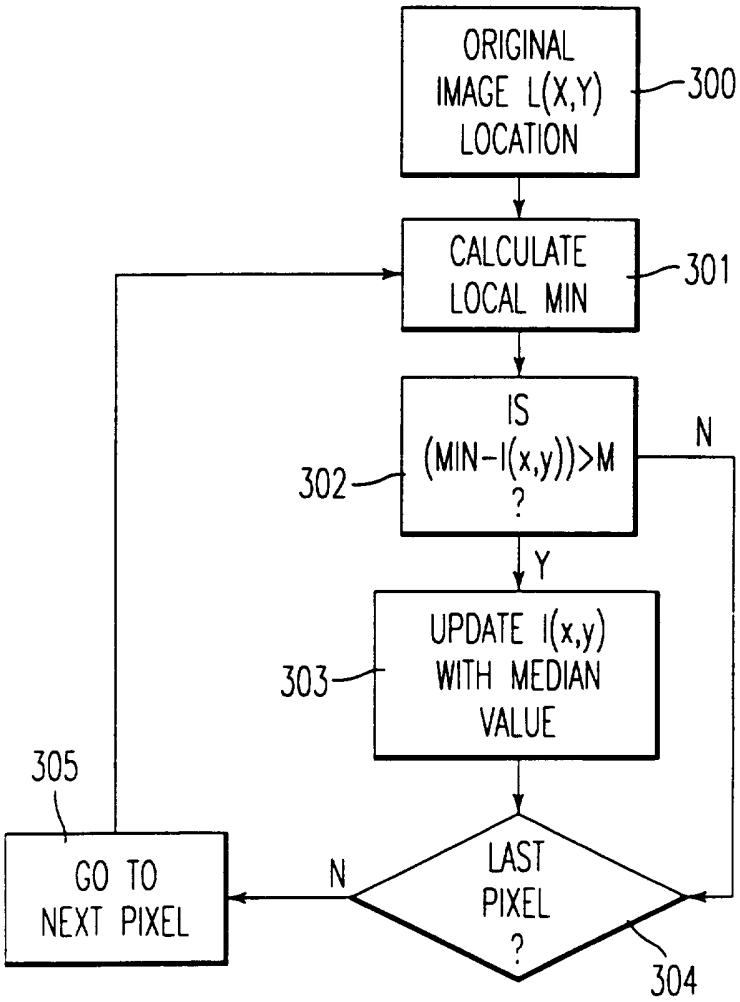
ORIGINAL IMAGE L(X,Y) LOCATION
300
CALCULATE LOCAL MIN
301
IS (MIN-I(x,y))>M ?
302
N
Y
UPDATE I(x,y) WITH MEDIAN VALUE
303
LAST PIXEL ?
304
N
GO TO NEXT PIXEL
305

FIG. 3A

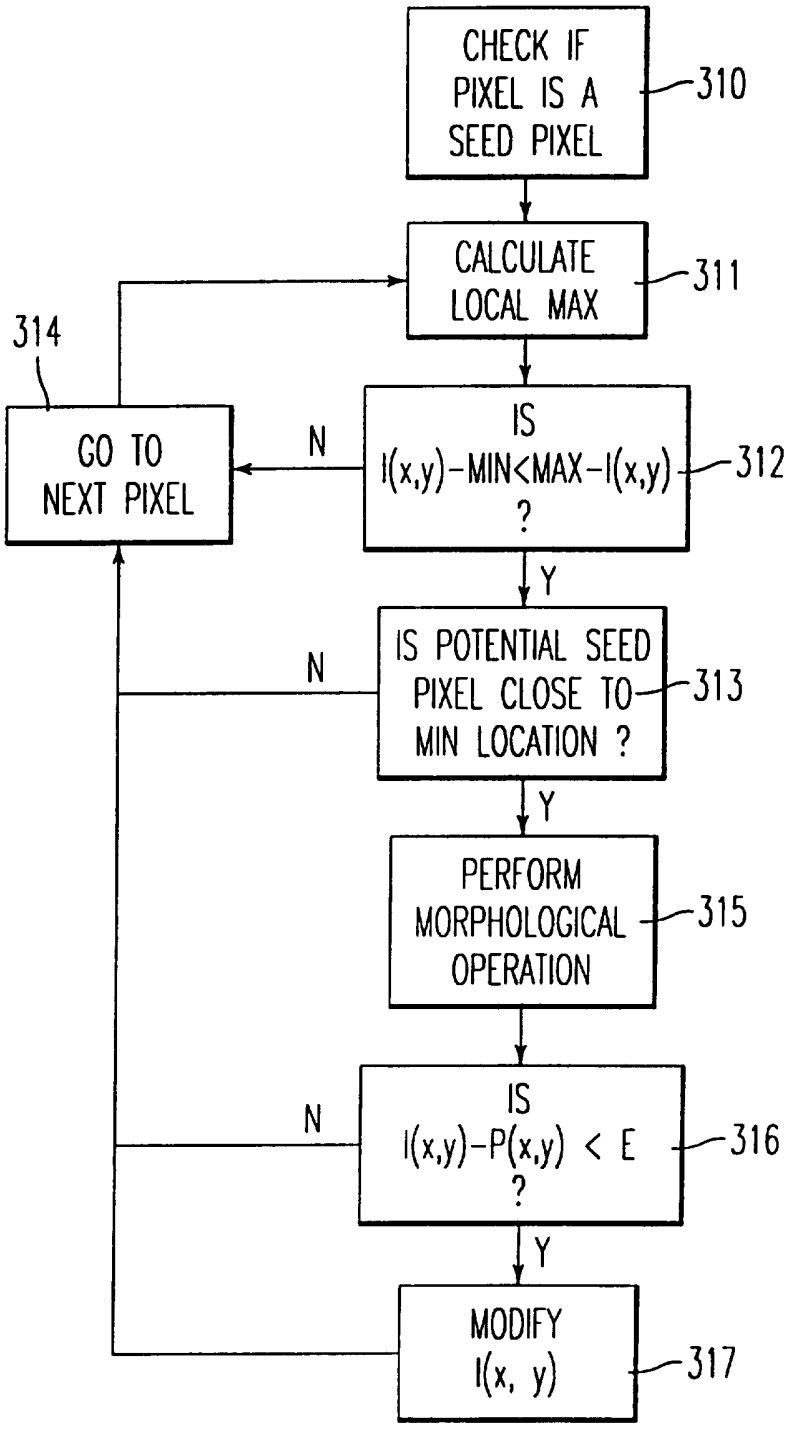
CHECK IF PIXEL IS A SEED PIXEL
310
CALCULATE LOCAL MAX
311
314
GO TO NEXT PIXEL
N
IS I(x,y)-MIN<MAX-I(x,y) ?
312
Y
N
IS POTENTIAL SEED PIXEL CLOSE TO MIN LOCATION ?
313
Y
PERFORM MORPHOLOGICAL OPERATION
315
N
IS I(x,y)-P(x,y) < E ?
316
Y
MODIFY I(x, y)
317

FIG. 3B

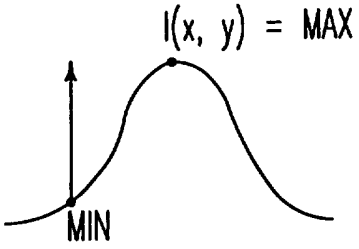

I(x, y) - MIN = L
MAX - I(x, y) = 0

FIG. 3C

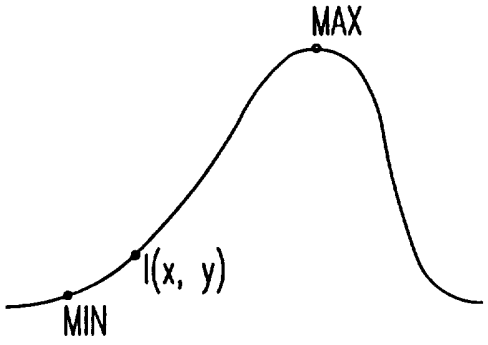

I - MIN < MAX - I

FIG. 3D

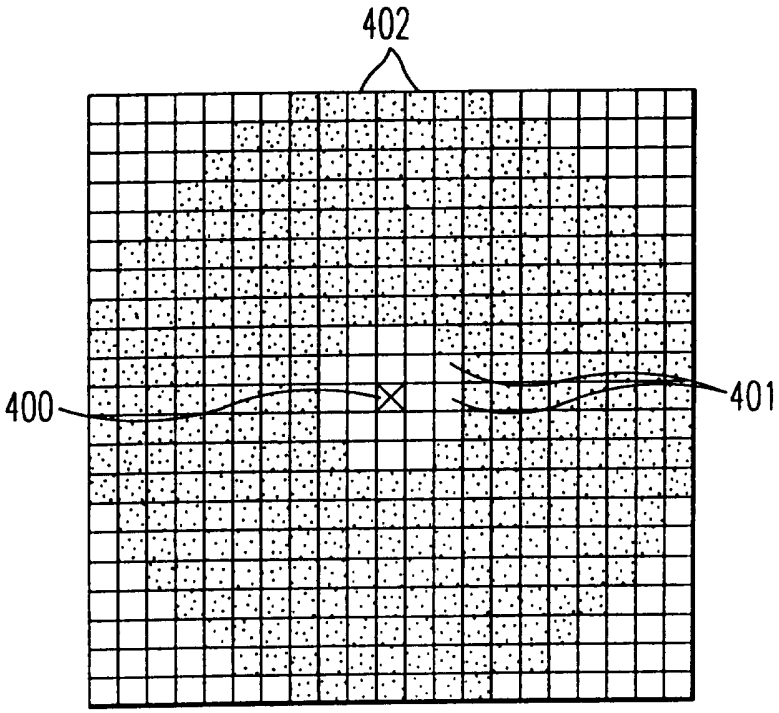

FIG. 4

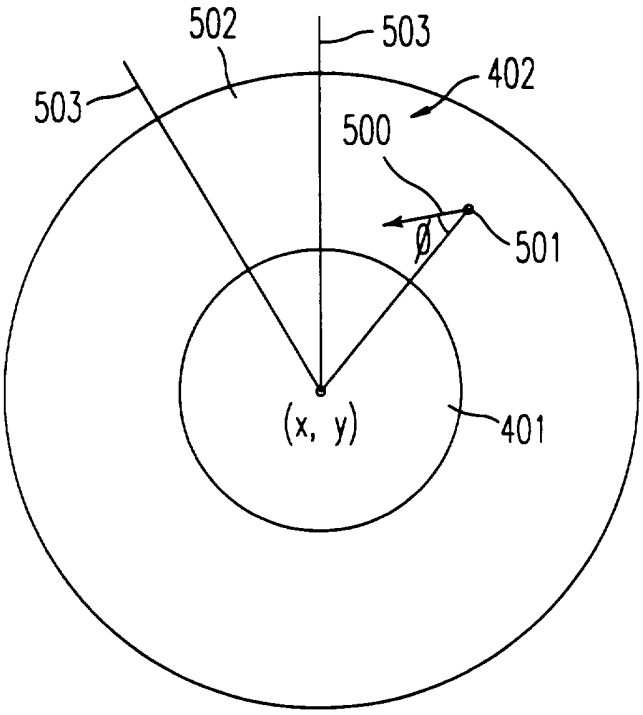

FIG. 5

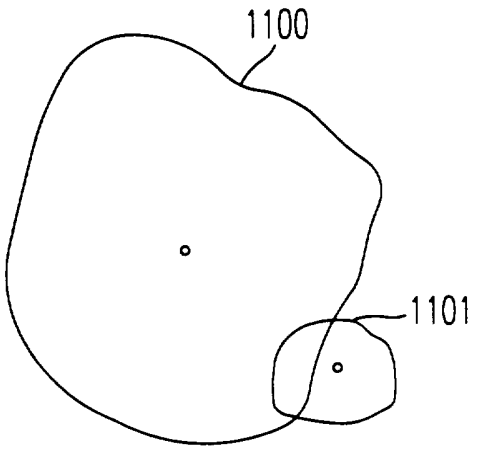

FIG. 11

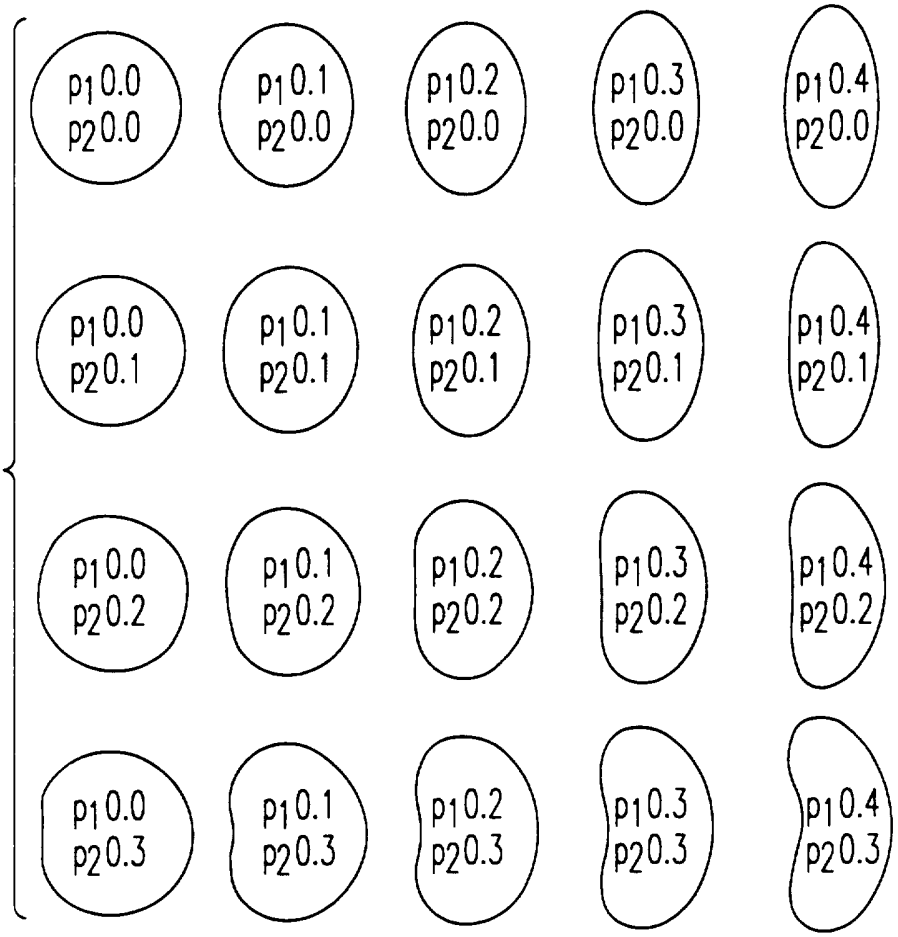
p1 0.0 p2 0.0
p1 0.1 p2 0.0
p1 0.2 p2 0.0
p1 0.3 p2 0.0
p1 0.4 p2 0.0
p1 0.0 p2 0.1
p1 0.1 p2 0.1
p1 0.2 p2 0.1
p1 0.3 p2 0.1
p1 0.4 p2 0.1
p1 0.0 p2 0.2
p1 0.1 p2 0.2
p1 0.2 p2 0.2
p1 0.3 p2 0.2
p1 0.4 p2 0.2
p1 0.0 p2 0.3
p1 0.1 p2 0.3
p1 0.2 p2 0.3
p1 0.3 p2 0.3
p1 0.4 p2 0.3

FIG. 6

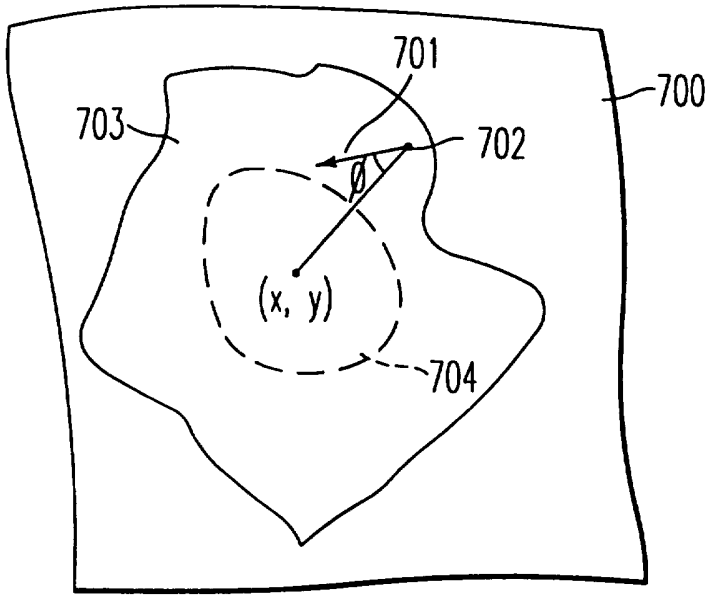
701
700
703
702
Ø
(x, y)
704

FIG. 7

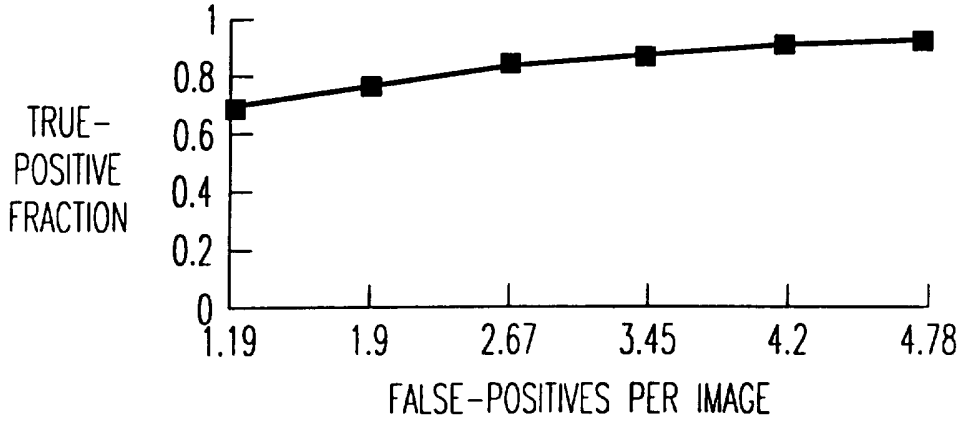
TRUE-
POSITIVE
FRACTION
1
0.8
0.6
0.4
0.2
0
1.19
1.9
2.67
3.45
4.2
4.78
FALSE-POSITIVES PER IMAGE

FIG. 16

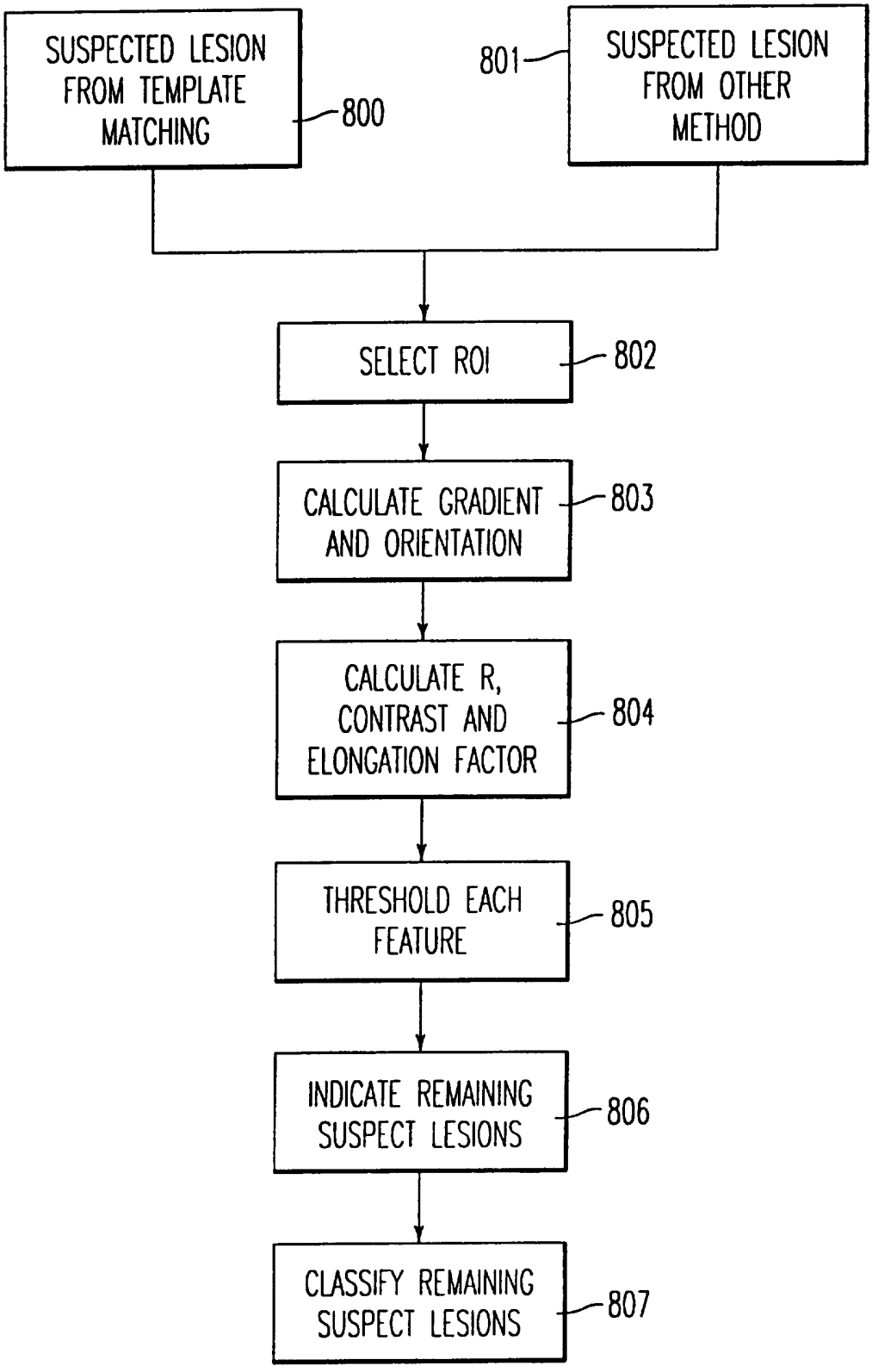
SUSPECTED LESION FROM TEMPLATE MATCHING
800
801
SUSPECTED LESION FROM OTHER METHOD
SELECT ROI
802
CALCULATE GRADIENT AND ORIENTATION
803
CALCULATE R, CONTRAST AND ELONGATION FACTOR
804
THRESHOLD EACH FEATURE
805
INDICATE REMAINING SUSPECT LESIONS
806
CLASSIFY REMAINING SUSPECT LESIONS
807

FIG. 8

PIXEL SIZE	DETECTED LESION SIZE
500 MICRON	4-10 mm
1000 MICRON	8-21 mm
2000 MICRON	16-42 mm
4000 MICRON	32-84 mm

FIG. 9A

KERNEL RADIUS (INNER; IN PIXELS)	KERNEL RADIUS (OUTER; IN PIXELS)	DETECTED LESION SIZE (mm)
3	12	4-10
6	24	8-21
12	48	16-42
24	96	32-84

FIG. 9B

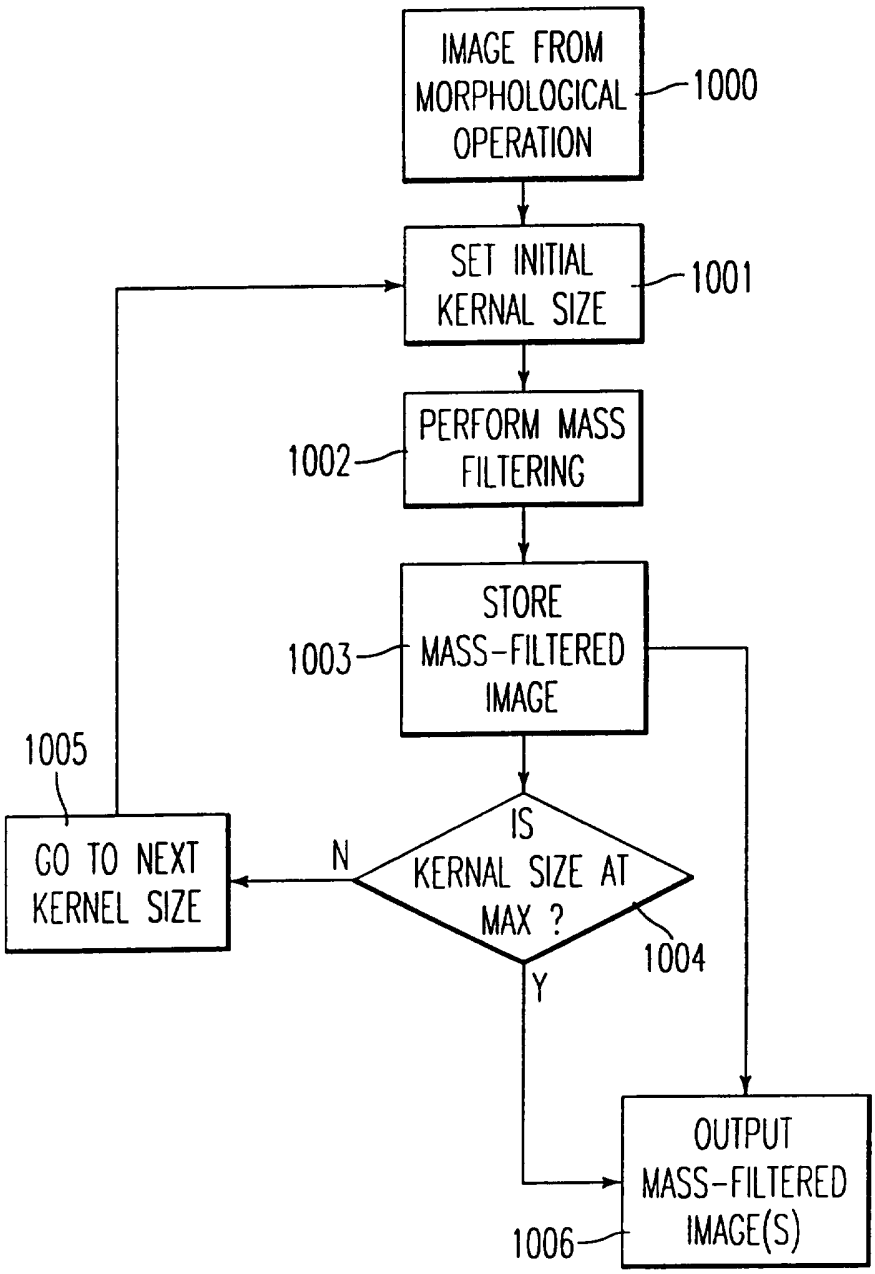
IMAGE FROM MORPHOLOGICAL OPERATION
1000
SET INITIAL KERNAL SIZE
1001
PERFORM MASS FILTERING
1002
STORE MASS-FILTERED IMAGE
1003
IS KERNAL SIZE AT MAX ?
1004
N
Y
GO TO NEXT KERNEL SIZE
1005
OUTPUT MASS-FILTERED IMAGE(S)
1006

FIG. 10

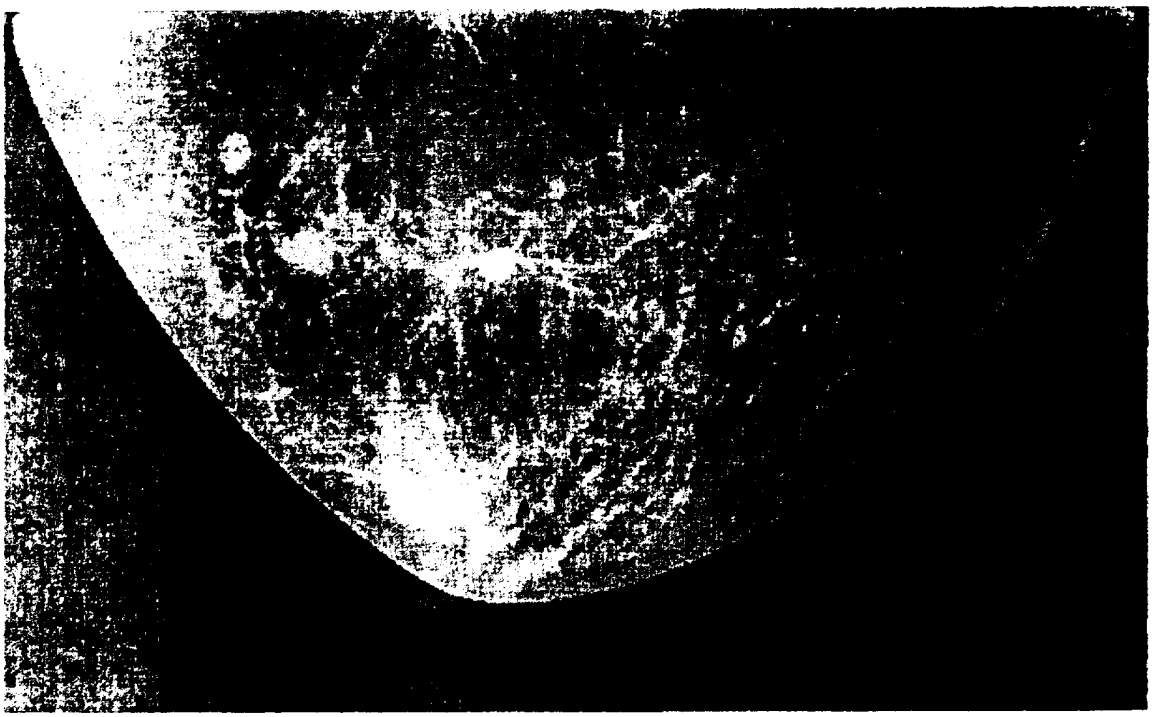

FIG.12B

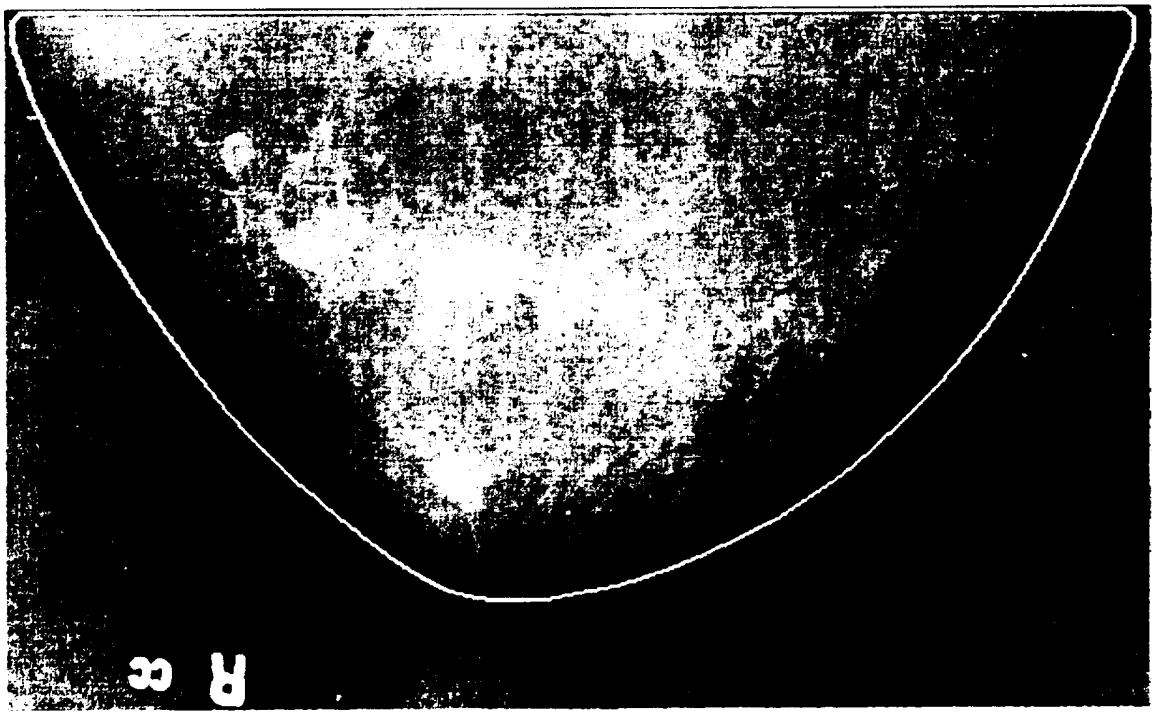

FIG.12A

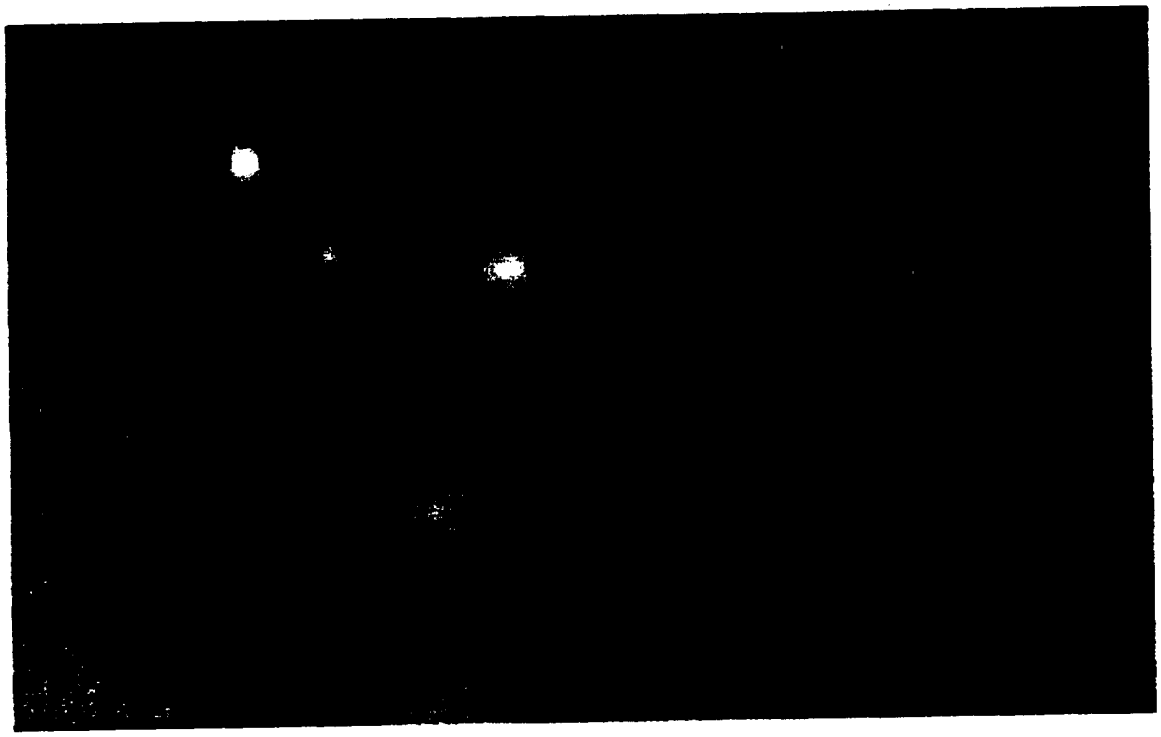

FIG.12D

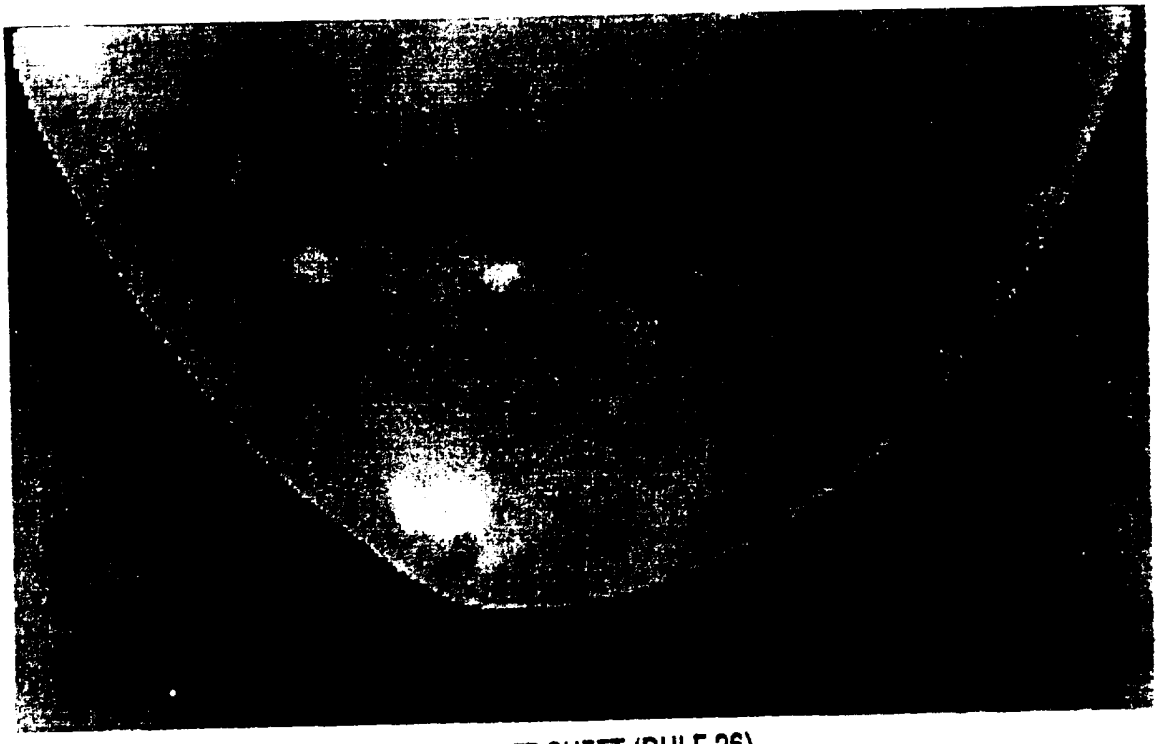

FIG.12C

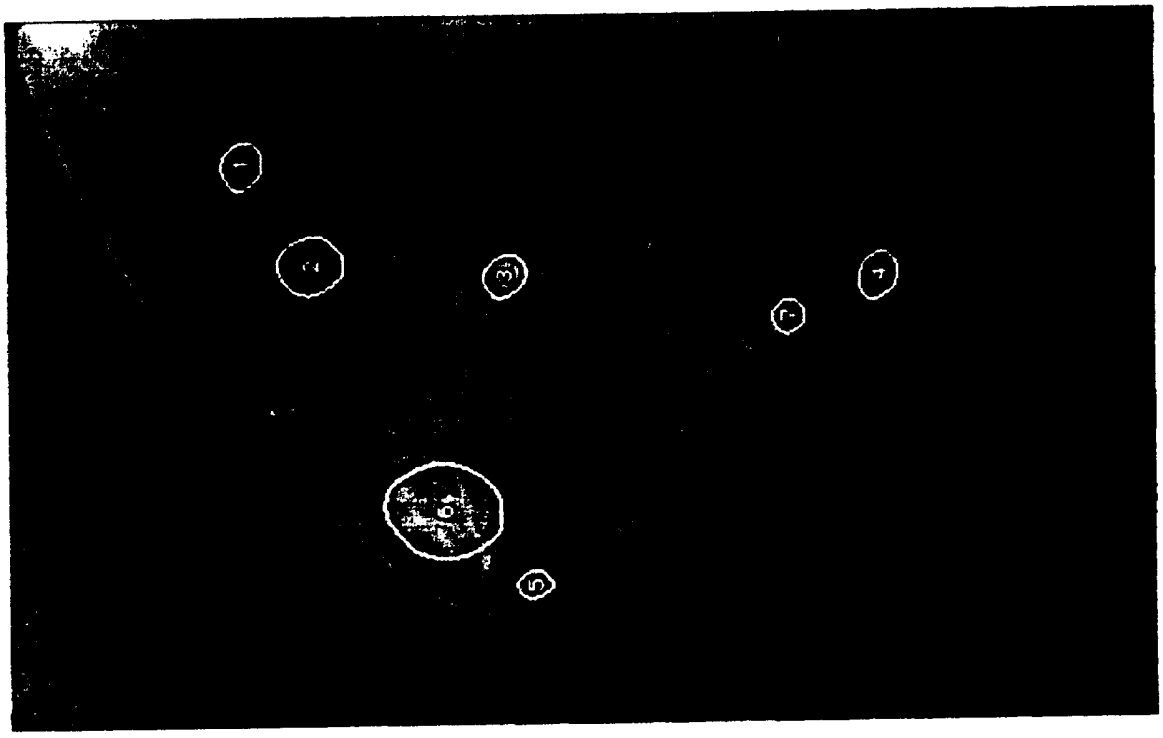

FIG.12F

FIG.12E

FIG. 13B

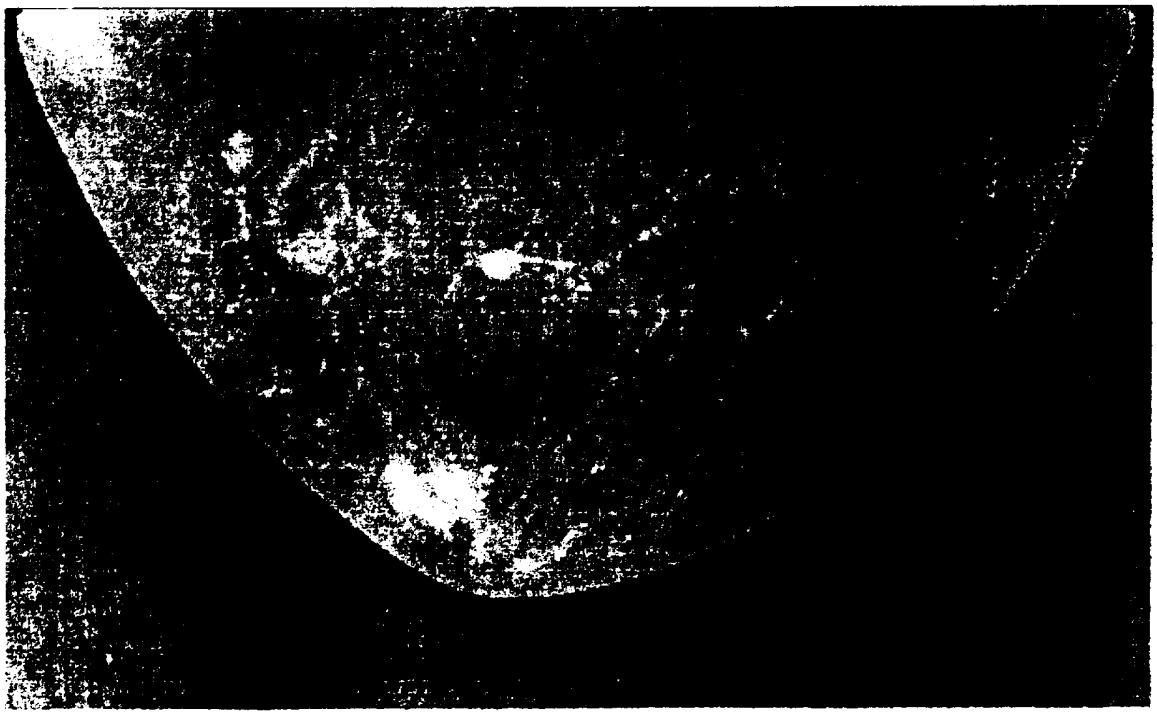

FIG. 13A

FIG.13D

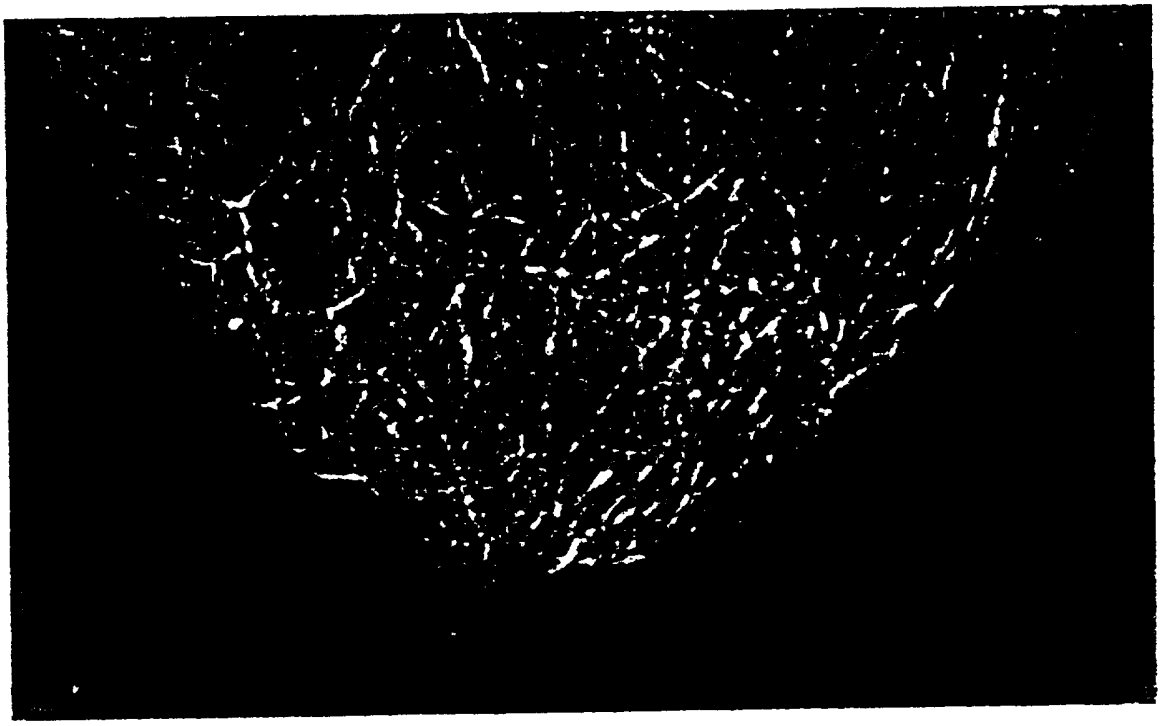

FIG.13C

FIG.13F

FIG.13E

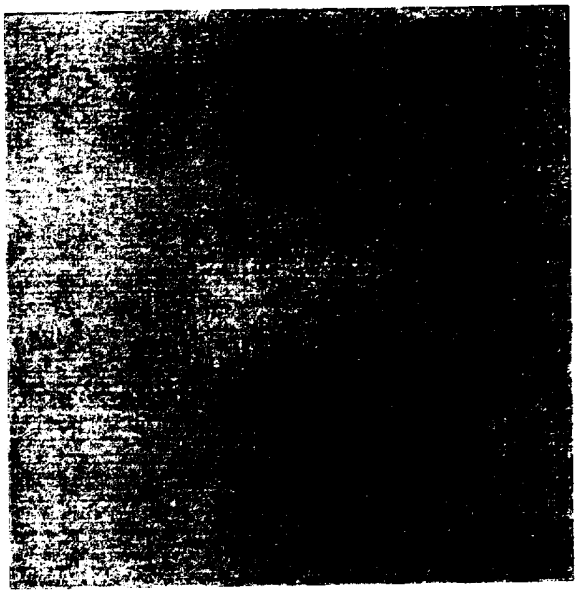

FIG.14A

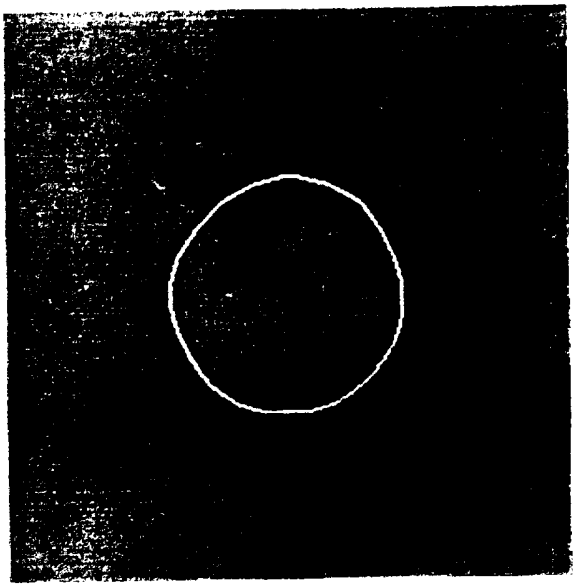

FIG.14B

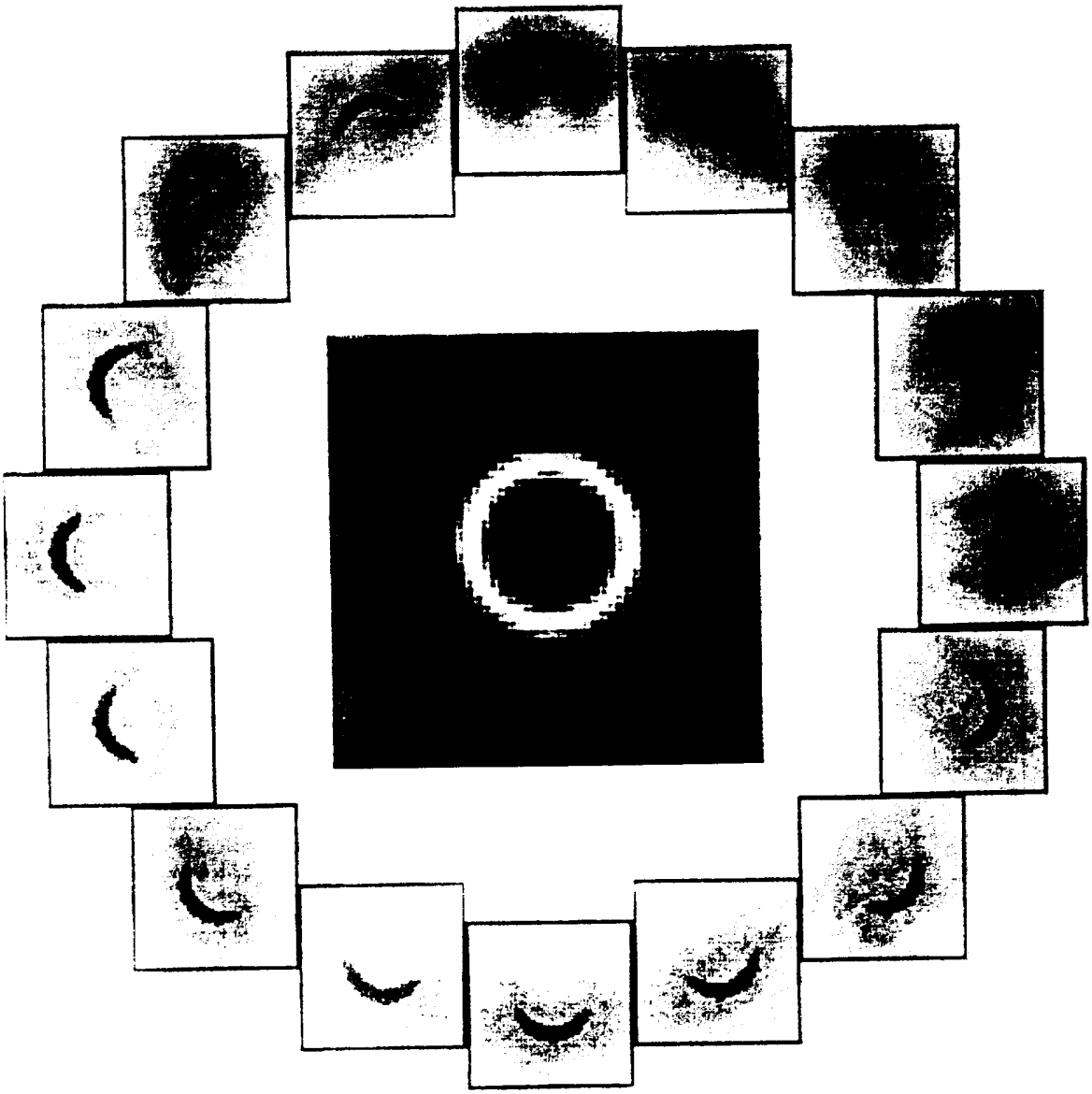

FIG.14C

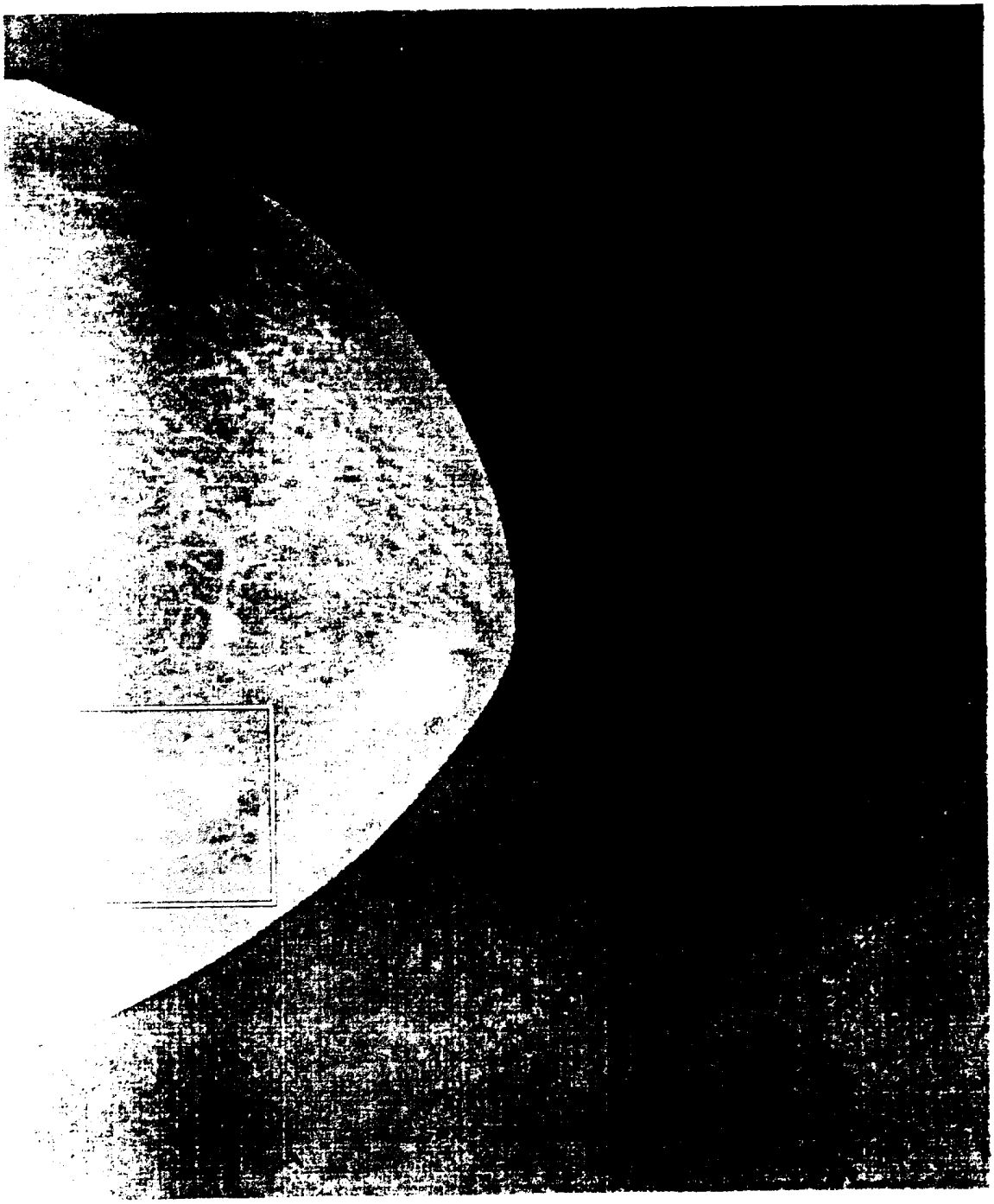

FIG.15A

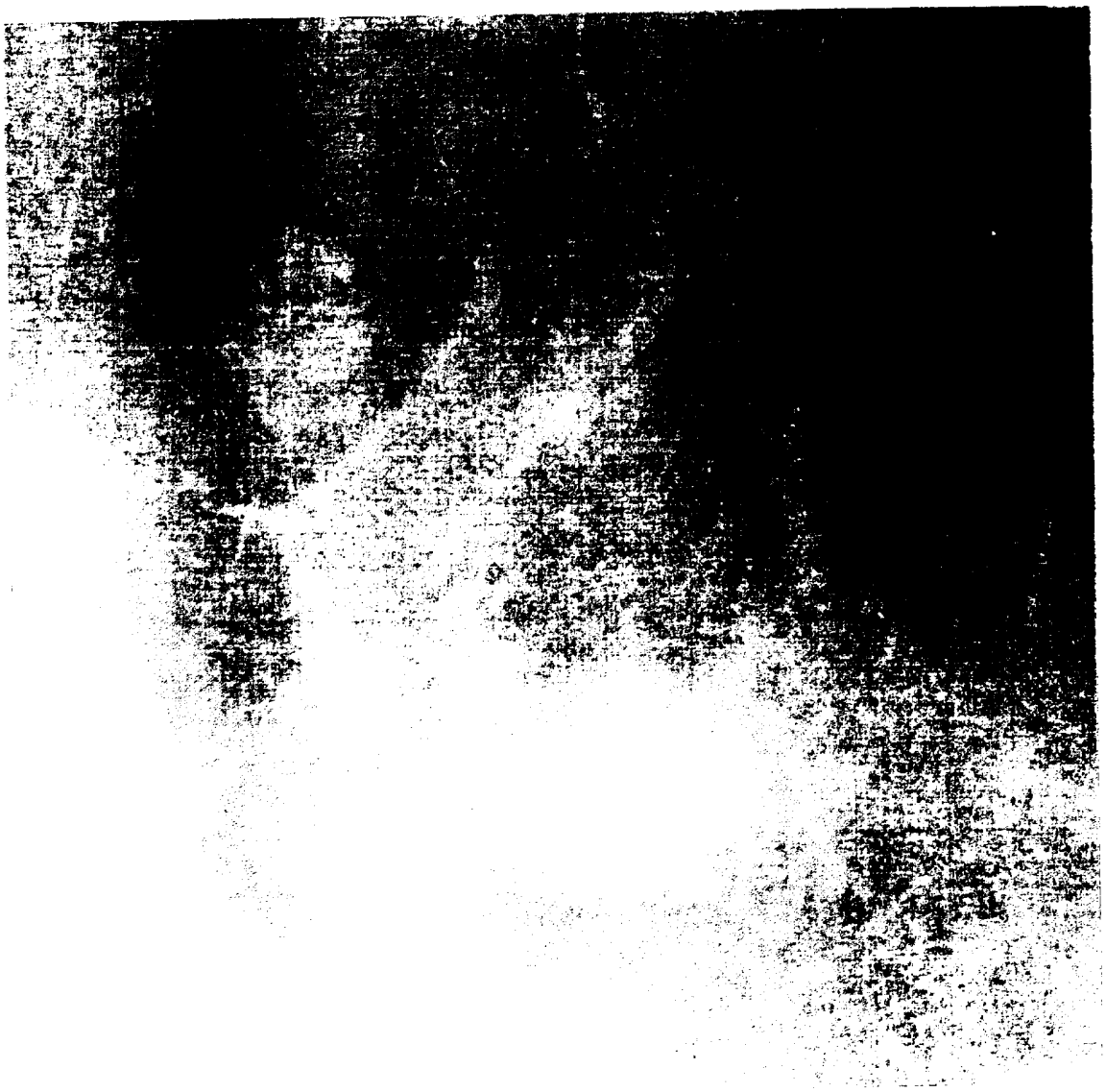

FIG.15B

FIG.15C

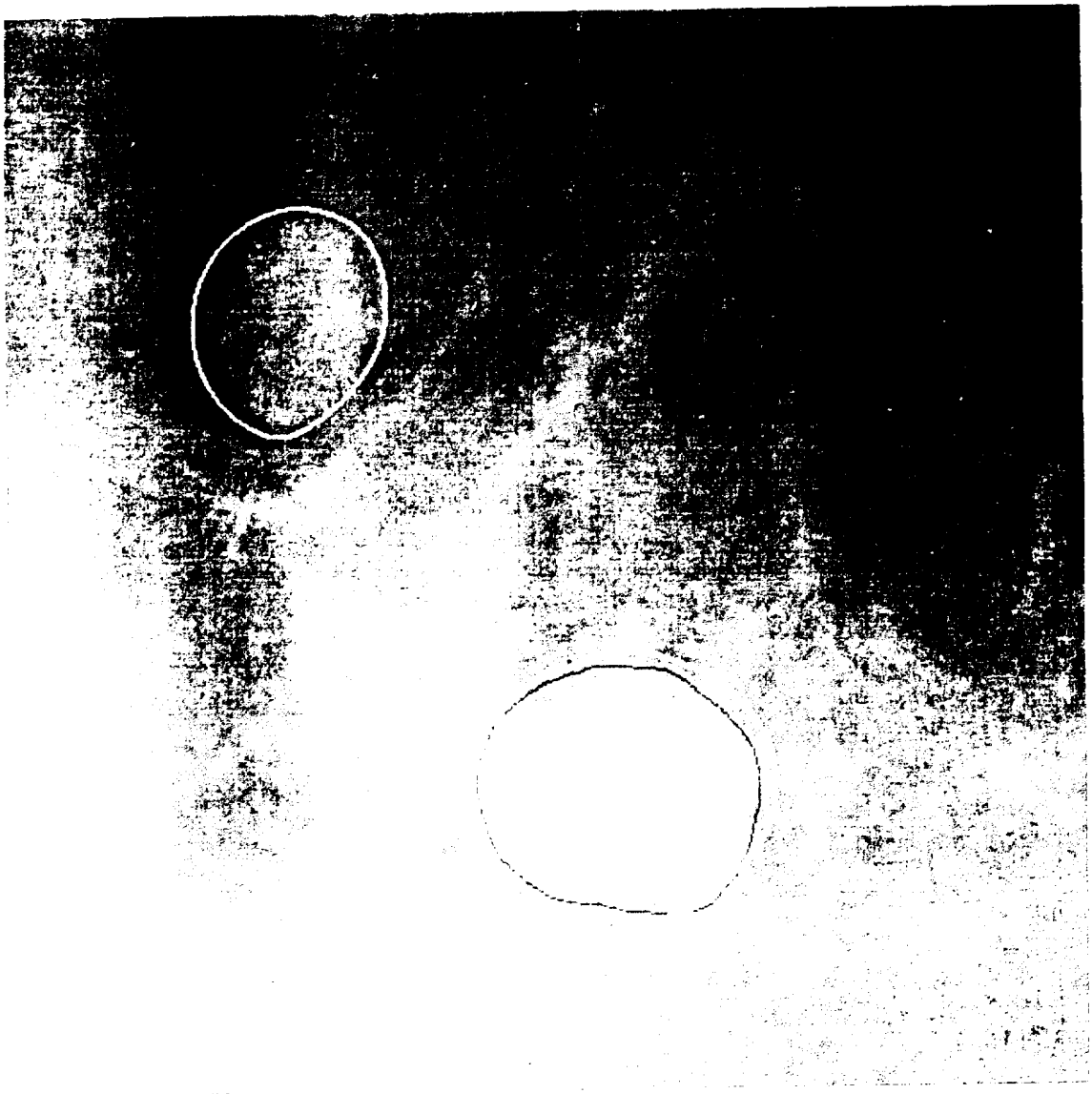

FIG. 15D

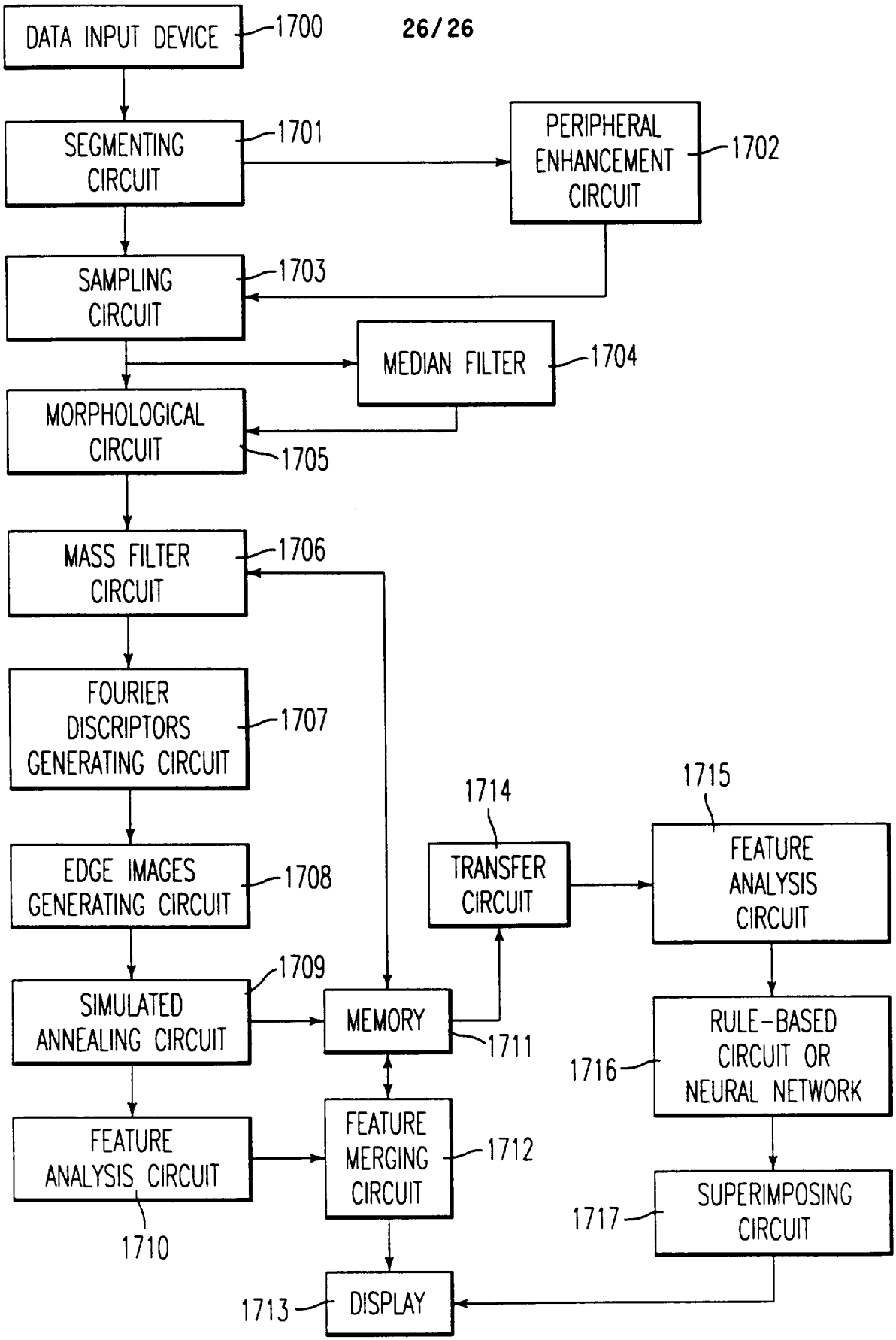
DATA INPUT DEVICE
1700
SEGMENTING CIRCUIT
1701
PERIPHERAL ENHANCEMENT CIRCUIT
1702
SAMPLING CIRCUIT
1703
MEDIAN FILTER
1704
MORPHOLOGICAL CIRCUIT
1705
MASS FILTER CIRCUIT
1706
FOURIER DISCRIPTORS GENERATING CIRCUIT
1707
EDGE IMAGES GENERATING CIRCUIT
1708
SIMULATED ANNEALING CIRCUIT
1709
MEMORY
1711
FEATURE ANALYSIS CIRCUIT
1710
FEATURE MERGING CIRCUIT
1712
DISPLAY
1713
1714
TRANSFER CIRCUIT
1715
FEATURE ANALYSIS CIRCUIT
RULE-BASED CIRCUIT OR NEURAL NETWORK
1716
SUPERIMPOSING CIRCUIT
1717

FIG. 17

INTERNATIONAL SEARCH REPORT

International application No.
PCT/US96/02439

A. CLASSIFICATION OF SUBJECT MATTER

IPC(6) :G06K 9/00
US CL :382/128000

According to International Patent Classification (IPC) or to both national classification and IPC

B. FIELDS SEARCHED

Minimum documentation searched (classification system followed by classification symbols)

U.S. : 382/130, 131, 132, 261, 298

Documentation searched other than minimum documentation to the extent that such documents are included in the fields searched

NONE

Electronic data base consulted during the international search (name of data base and, where practicable, search terms used)

APS: Searched Terms: mammograph, mass filter, lesion, morphological

C. DOCUMENTS CONSIDERED TO BE RELEVANT

Category*	Citation of document, with indication, where appropriate, of the relevant passages	Relevant to claim No.
Y	US,A 5,133,020 (GIGER ET AL.) 21 July 1992, Figure 19, element 600; column 10, lines 30-40; column 12, lines 20-46; column 6, lines 6-7; figure 2, element 180;	1
Y	US, A, 4,907,156 (DOI ET AL.) 06 MARCH 1990, column 14, lines 46-68;	1
X	US, A 5,016,173 (KENET ET AL.) 14 May 1991, Abstract	1
X	US,A 5,359,513 (KANO ET AL.) 25 October 1994, Figure 1B	1
X	US,A 5,432,865 (KASDAN ET AL.) 11 July 1995, Figure 1	1

☐ Further documents are listed in the continuation of Box C. ☐ See patent family annex.

*	Special categories of cited documents:	"T"	later document published after the international filing date or priority date and not in conflict with the application but cited to understand the principle or theory underlying the invention
"A"	document defining the general state of the art which is not considered to be part of particular relevance	"X"	document of particular relevance; the claimed invention cannot be considered novel or cannot be considered to involve an inventive step when the document is taken alone
"E"	earlier document published on or after the international filing date	"Y"	document of particular relevance; the claimed invention cannot be considered to involve an inventive step when the document is combined with one or more other such documents, such combination being obvious to a person skilled in the art
"L"	document which may throw doubts on priority claim(s) or which is cited to establish the publication date of another citation or other special reason (as specified)	"&"	document member of the same patent family
"O"	document referring to an oral disclosure, use, exhibition or other means		
"P"	document published prior to the international filing date but later than the priority date claimed		

Date of the actual completion of the international search 08 APRIL 1996	Date of mailing of the international search report 23 APR 1996
Name and mailing address of the ISA/US Commissioner of Patents and Trademarks Box PCT Washington, D.C. 20231 Facsimile No. (703) 305-6606	Authorized officer MICHAEL T. RAZAVI Telephone No. (703) 305-4713

Form PCT/ISA/210 (second sheet)(July 1992)*